JOURNAL OF MATERIALS SCIENCE 21 (1986) 3050–3064

The effects of amorphous phase separation on crystal nucleation kinetics in $BaO–SiO_2$ glasses

Part 3 *Isothermal treatments at 718 to 760° C; small-angle X-ray scattering results*

E. D. ZANOTTO*, P. F. JAMES
Department of Ceramics, Glasses and Polymers, University of Sheffield, Sheffield S10 2TZ, UK
A. F. CRAIEVICH
Centro Brasileiro de Pesquisas Físicas, CNPq, Rua Xavier Sigaud 150, 22290 Rio de Janeiro, Brazil

The nucleation kinetics of barium disilicate spherulites were determined by optical microscopy in $BaO–SiO_2$ glasses containing 27.0 to 33.3 mol % BaO for isothermal treatments at 718 to 760° C. Amorphous phase separation in two glasses was studied by small-angle X-ray scattering (SAXS) and transmission electron microscopy (TEM). The average diameter, number and surface area of amorphous droplets were obtained by SAXS as a function of time at 743 and 760° C. In glasses not showing amorphous phase separation the crystal nucleation rate, *I*, was constant at a given temperature. In glasses undergoing phase separation, *I* increased with time approaching a constant value, which was identical for different phase-separated glasses. There was a striking correlation between the time to reach a constant *I* and the time required to attain the equilibrium composition of the amorphous (baria-rich) matrix phase, as revealed by a constant integrated SAXS intensity. The crystal nucleation rate, *I*, depended primarily on the composition of the baria-rich phase. There was no apparent relationship between *I* and the surface area or number of droplets from SAXS. However, possible evidence of additional crystal nucleation at droplet interfaces was found, although the effect was small. Viscosities and crystal growth rates for the phase-separated glasses are also discussed.

1. Introduction

Glass ceramics are an important class of materials made by the controlled crystallization of glasses. Many glass compositions exhibit amorphous phase separation prior to crystal nucleation and growth during the heat-treatment schedule required to convert them to glass ceramics. It has long been recognized that there may be a link between amorphous phase separation and crystal nucleation and growth in glasses and there is evidence that in certain complex compositions phase separation promotes high volume nucleation and consequently the formation of fine grain glass ceramics. However, in spite of numerous studies the role of phase separation remains a matter of debate (see, for example, [1–4]).

In the present work an attempt is made to clarify the role of phase separation in glass ceramic formation. The $BaO–SiO_2$ system was selected for intensive study since it has several ideal features. It has an extensive region of sub-liquidus immiscibility and exhibits internal (volume) nucleation of the $BaO \cdot 2SiO_2$ crystalline phase without deliberate additions of nucleation catalysts, which simplifies interpretation of the results. Also the crystal nucleation rates are relatively high, but not too high, to be conveniently measured.

In Part 1 of the present series [5] previous work on the $BaO–SiO_2$ and other systems was reviewed and the possible effects of phase separation on crystal nucleation were discussed. These effects were broadly classified as "compositional" or "interfacial". In the former case, crystal nucleation occurred within one of the amorphous phases and was determined by its composition; in the latter case, it was assumed to occur preferentially (for various reasons) at the interfaces between the phases. The kinetics of crystal nucleation of barium disilicate were studied in a series of $BaO–SiO_2$ glasses ranging from 25.3 to 33.1 mol % BaO, a constant nucleation time of 1 h being used for each glass at temperatures from 673 to 807° C. The highest nucleation rates were observed in the 33.1 mol % BaO glass close to the $BaO \cdot 2SiO_2$ composition, which was just outside the immiscibility region. Lower rates were found in the glasses with lower BaO contents including those exhibiting amorphous phase separation. However, it was deduced that phase separation had a marked but indirect effect on

*Present address: Departamento de Engenharia de Materiais, Universidade Federal de São Carlos, Caixa Postal 676, 13560 São Carlos, SP, Brazil.

0022–2461/86 $03.00 + .12

crystal nucleation because of the accompanying shift in composition of the baria-rich phase in which crystal nucleation occurred, so that after phase separation at a given temperature the crystal nucleation rates of different glasses tended to converge to similar values. There was no evidence for a significant enhancement of crystal nucleation at the interfaces between the amorphous phases.

In Part 2 of this series [6] several of the glasses (containing 25.3, 28.5 and 30.4 mol % BaO) were explored in greater detail. The crystal nucleation kinetics and development of amorphous phase separation were followed simultaneously for isothermal treatment at 700° C. Quantitative measurements of phase separation were obtained by replica electron microscopy, the nucleation kinetics being determined by optical microscopy, as in Part 1. In the 25.3 and 28.5 glasses, which phase separated, the rates of crystal nucleation were profoundly influenced by the phase separation. Marked differences in crystal nucleation rates occurred at 700° C depending on the nature of the previous heat treatment given to each glass, for example whether the glass had been heat treated to a higher temperature to induce phase separation or whether it had been rapidly cooled to suppress phase separation. Moreover, at 700° C phase separation and crystal nucleation occurred simultaneously over an extended period producing an increase in crystal nucleation rate with time, which was manifested in curved plots of N_v (number of crystals per unit volume) against time. In contrast, for glass 30.4, which did not phase separate at 700° C, the plots were linear. All the observed effects of phase separation on crystal nucleation could be clearly explained in terms of the composition of the baria-rich matrix phase. Crystal nucleation rates rose with increase in baria content, the highest rate being observed at the barium disilicate composition. Prior heat treatments produced major shifts in composition of the phases. Also, at 700° C the average baria content of the baria-rich phase increased gradually towards the equilibrium value given by the immiscibility boundary. Finally, in these experiments the interface between the amorphous phases did not appear to affect the crystal nucleation rates significantly.

In Part 3 the isothermal studies have been extended to higher nucleation temperatures from 718 to 760° C, to test further the explanations put forward in Parts 1 and 2. As before, the crystal nucleation kinetics were determined by quantitative optical microscopy. These results were correlated with quantitative data from small-angle X-ray scattering (SAXS) on the kinetics of amorphous phase separation. Information on various morphological parameters of the phase separation were obtained including average size and numbers of droplets, surface area of the dispersed phase and the degree of separation, as determined from the integrated intensity, Q. The SAXS method was more accurate than the electron microscope replica technique used to characterize the phase separation in Part 2, and was particularly useful in assessing the time required for the phases to achieve their equilibrium compositions (using Q). While the primary objective remained to relate crystal nucleation to phase separation the SAXS results on the kinetics of phase separation were of considerable interest in their own right and were compared with data from transmission electron microscopy (TEM) of thin sections of the glasses. Results on the affects of phase separation on viscosity and crystal growth rates were also obtained. Finally, a vital part of the work was to ensure that the glasses were as chemically homogeneous as possible, their compositions were known accurately and that their impurity levels were fully characterized.

2. Experimental details

2.1. Preparation of glasses and chemical analysis

A series of $BaO-SiO_2$ glasses were prepared in the range 27.0 to 33.3 mol % BaO. Each glass was given a code number, e.g. 28.3 A, the number indicating the mol % BaO from chemical analysis and the letter designating a particular melt. Efforts were made to minimize impurity levels in the glasses by careful choice of starting materials because of the possible effects these might have on the nucleation rates. The starting materials were Silquartz (99.99 wt % SiO_2) and $BaCO_3$ (Fisons AR grade for glasses 27.0, 28.3 A, 28.3 B, 29.9 and 33.3 A; BDH Analar grade for glass 29.7). Batches of 150 to 250 g were melted in platinum-rhodium crucibles in electrical furnaces at 1550°C. To ensure homogeneity of the glasses a special procedure was used. This differed from that described in Part 1, but was equally effective. First, the batches were sintered in platinum dishes at 1300° C for 24 h prior to melting. After melting and pouring, the glasses were crushed and remelted from four to eight times. Finally the melts were cast and pressed between steel plates. Clear samples, 1 to 2 mm thick, were obtained. Specimens for viscosity determinations were cast in graphite cylinders with diameters of 20 to 30 mm and transferred to an annealing furnace maintained at 400° C. The furnace was then switched off and the specimens allowed to cool slowly overnight. No internal crystallization was observed after this treatment.

All the glasses and starting materials were given a complete analysis for BaO, SiO_2 and likely impurities, since a thorough characterization of the glasses was most important to the work. Full details of the methods and results are given in [7]. A summary of the main results are presented in Table I. The SiO_2 and BaO contents were determined either by wet chemistry techniques or by electron probe microanalysis (EPMA). Good agreement was obtained between these methods. The impurity elements were determined by flame emission spectroscopy (FES) and/or atomic absorption spectroscopy (AAS).

The SiO_2, BaO and SrO contents of the glasses from chemical analysis were close to the nominal contents calculated from the chemical analysis of the batch materials (Table I). The main impurity was SrO, the source being the $BaCO_3$. The Fisons and BDH $BaCO_3$ contained approximately 0.4 and 0.7 wt % SrO, respectively, from analysis. The levels of other impurities in the $BaCO_3$ were very low (< 0.01 wt %). X-ray fluorescence analysis indicated very low impurity

TABLE I Chemical analysis (wt %) of glasses studied

	Glass 27.0		Glass 28.3A (28.3 B similar)			Glass 29.7			Glass 29.9		Glass 33.3A (33.2 B similar)		
	N	A	N	A		N	A		N	A	N	A	
SiO_2	50.66	–	49.54	49.3(P)		47.61	47.0	47.5(P)	47.60	–	43.6	43.1	
BaO	49.04	48.5	50.14	50.1	49.9(P)	51.90	51.8	51.4(P)	52.08	52.1	56.05	56.0	56.15(P)
SrO	0.29	0.26	0.29	0.27	0.33(P)	0.48	0.54	0.61(P)	0.30	0.28	0.33	0.29	0.33(P)
CaO	0.005	0.015	–	0.034		–	0.014		–	0.023	–	0.038	0.034(P)
Na_2O	0.005	–	–	0.011		–	0.013		–	–	–	0.007	0.12(P)
K_2O	0.008	0.027	–	0.023		–	0.012		–	0.024	–	0.026	0.021(P)
Al_2O_3	0.001	–	–	–		–	–		–	–	–	–	0.056(P)
Fe_2O_3	0.001	–	–	0.005		–	0.009		–	–	–	0.001	< 0.035(P)

N, nominal composition (wt %) calculated from batch materials.
A, analysis (wt %) of glass.
P, electron probe microanalysis of glass.
Glass code (e.g. 27.0) gives mol % BaO from analysis.

levels in the silica (Silquartz) (Na_2O 0.005 wt %, other impurities < 0.002 wt %). Apart from SrO the levels of impurities in the glasses were low (Table I), although higher than the levels expected from the analysis of the batch materials (given for glass 27.0 only in Table I, the values for the other glasses being similar). This implies some slight uptake of impurities during melting. The Al_2O_3 and Li_2O impurity levels were below the detection limits for AAS (i.e. 0.05 and 0.002 wt %, respectively). Platinum and TiO_2 levels were also below the EPMA limits (0.05 and 0.07 wt %, respectively).

As the main impurity was SrO the possible effects of this oxide on crystal nucleation in the glasses was of some interest. An experiment to test for such effects has been reported elsewhere by Zanotto and James [8]. They melted a barium disilicate glass (33.3 P) from extremely high purity starting materials (the glass contained 33.3 mol % BaO and only 0.004 wt % SrO). The nucleation rates in this glass were about 1.5 times higher than in glass 33.3 A used in this study, which contained about 0.3 wt % SrO. Clearly variations in SrO content cause significant changes in nucleation. However, the glasses used in the present work had nearly identical SrO contents (with the one exception of glass 29.7 which was prepared from a different $BaCO_3$). Thus the effect of SrO on nucleation would be almost the same for each glass. Since comparisons were being made between glasses and the predominant effects were caused by changes in BaO content the influence of SrO could thus be safely neglected.

Another possible impurity of some interest is "water" since it is well established that the presence of "water" or hydroxyl groups can affect crystal nucleation and growth in glasses [9]. Thin polished specimens of several of the glasses were prepared, "dried" at 400° C for several hours and examined by infrared transmission spectroscopy. The detailed results are given in [7]. Some absorption due to traces of water was detected. No exact quantitative determination of water content could be made because the extinction coefficients were not available. However, a rough estimate of the water content would be 0.01 to 0.02 wt %, as typically found in other silicate glasses [9]. This level would be expected to have only a minor effect on nucleation and growth in these glasses. Moreover, the water levels were very similar in all the glasses studied.

2.2. Determination of crystal nucleation kinetics

Glass specimens of about 3 × 3 × 1 mm^3 were heat treated to induce amorphous phase separation (where appropriate) and crystal nucleation at various temperatures from 718 to 760° C for different periods of time and air quenched. The same samples were given a crystal growth or "development" treatment at 810 to 830° C for 10 to 30 min to grow the crystal nuclei formed at the lower nucleation temperature to a sufficient size to be observed in an optical microscope. The method is fully discussed elsewhere [1, 5]. In the range of development temperatures the nucleation of new crystals was negligible. For some specimens, which were subjected to long periods of heat treatment, crystals could be observed after a single stage treatment. Heat treatments were performed in electric tube furnaces maintained to within 0.5° C. The temperature was measured by a Pt/13Rh thermocouple placed close to the samples. The thermocouple readings were checked carefully against a standard thermocouple.

The heat-treated specimens were mounted on glass plates with Canada Balsam, ground flat to remove any surface crystallization and polished with cerirouge. An etching of 10 to 15 sec in a 0.6 HF 0.2 HCl (vol %) solution was sufficient to reveal spherulites of the barium disilicate crystal phase. Photographs were taken with a Zeiss ultraphot 2 microscope with 16 × or 40 × objectives depending on the sizes of the crystals. The magnification on the final prints was obtained by means of a calibrated graticule which was photographed in the same microscope. From 200 to 800 crystalline particles (spherulites) were counted and measured in each sample. The number of crystal spherulites per unit volume, N_v (equal to the number of nuclei per unit volume after the first stage heat treatment) was then determined by the standard method discussed in Part 1 [5]. Optical micrographs of the spherulites were very similar to those shown earlier [5, 6]. The statistical error in N_v was ± 10 to 20% (95% confidence limits), depending on the size distribution of crystals and number of crystals measured. Another systematic source of error arose from failure to observe on the sections a fraction of the particles which were below the resolution limit of the optical microscope. This led to a small systematic

underestimation of the N_v values by between 3 and 14%, depending on the particle size distribution involved. This was not a serious error and had no appreciable effect on the results. A complete mathematical treatment of these errors is given in [7].

It was most important that the glasses were chemically homogeneous. Tests showed that N_v was constant throughout the heat-treated samples apart from the expected statistical variation mentioned above. This indicated that the crushing/remelting technique produced highly homogenous glasses.

2.3. Determination of the kinetics of amorphous phase separation by small-angle X-ray scattering (SAXS)

The X-ray intensity against scattering angle curves were obtained using a Rigaku X-ray generator and small-angle goniometer with slit collimation. The Cu$K\alpha$ radiation was isolated by means of a graphite monochromator in the scattered beam. The intensities were determined using a scintillation detector and a step scanning device. A slit system provided a "linear" beam. The cross section of the beam had negligible width and was taken as "infinitely high" [10], a condition that was satisfied for the specimens studied. The experimental scattering curves were corrected for parasitic scattering and normalized to a constant sample thickness and equivalent incident X-ray beam intensity. Full details are given elsewhere [7]. The optimum thickness for the $BaO-SiO_2$ glasses studied is approximately 16 μm. The actual samples used were ground and polished to approximately $20 \times 6 \times 0.03\,mm^3$ because it was difficult to obtain specimens thinner than 30 μm having such a relatively large area.

The intensity of X-rays scattered at small angles by an isotropic system containing a low concentration, N, of random identical particles of uniform electronic density is given by the Guinier equation [11],

$$I(s) = I_e N(\Delta\varrho)^2 v^2 \exp[-4\pi^2 s^2 Rg^2/3] \quad (1)$$

where s is the modulus of the scattering vector in reciprocal space which is related to the scattering angle ε by $(2/\lambda)\sin(\varepsilon/2)$ where λ is the X-ray wavelength (at small angles s is approximately ε/λ); I_e is the intensity scattered by a free electron; $\Delta\varrho$ is the difference between the electronic densities of the particles and matrix; v is the volume of a particle; and Rg is the radius of gyration of the particles (for spherical homogeneous particles $Rg = (3/20)^{1/2} D$ where D is the particle diameter). Thus from the slope of a log $I(s)$ against s^2 plot at very small angles Rg, and hence D, may be determined.

At larger scattering angles, Equation 1 is no longer valid. The intensity in the limit of large scattering angles (large s) may be represented by Porod's law [12–14]

$$I(s)\ (s \to \infty) = I_e (\Delta\varrho)^2 S'/8\pi^3 s^4 \quad (2)$$

where S' is the total surface area of the particles. This equation assumes a two-phase system in which the particles and matrix have uniform electronic densities, the particles have well-defined interfaces, are randomly orientated and have any shape except that of needles or plates.

The integrated SAXS intensity in reciprocal space, Q, is given by [11]

$$Q = 4\pi \int_0^\infty I(s)\, s^2 ds \quad (3)$$

For a two-phase system it can be shown that [11]

$$Q \propto \phi_1(1 - \phi_1)\,(\Delta\varrho)^2 \quad (4)$$

where ϕ_1 is the volume fraction occupied by the particles and $\Delta\varrho$ the electron density difference between particles and matrix, is related to the difference in composition between phases. Using Q it is possible to determine whether phase separation is at an early stage as, for example, when nucleation and growth of amorphous droplets is occurring during isothermal treatment. In this case Q increases with time. However, if Q becomes constant after a certain period of isothermal treatment the amorphous phase separation is in the final stage when the volume fractions and compositions of the droplets and matrix have reached equilibrium, although the larger droplets will continue to grow at the expense of the smaller ones, i.e. coarsening will occur.

From the experimental SAXS intensity, $J(s)$, measured by using a linear beam having a narrow and "infinitely high" cross section [10], the parameters Rg, S' and Q (Equations 1, 2 and 3) can be obtained directly. Equation 1 also holds as a good approximation for $J(s)$ at very small angles. Thus Rg can be determined from Guinier plots (log J against ε^2). Porod's law (Equation 2) becomes for $J(s)$ [11]:

$$J(s)\ (s \to \infty) = I_e(\Delta\varrho)^2 S'/16\pi^2 s^3 \quad (5)$$

The integral Q can be obtained from $J(s)$ by [11]:

$$Q = 2\pi \int_0^\infty J(s)\, s\, ds \quad (6)$$

The total surface area of the particles per unit volume, S_v (S'/V where V is the total volume irradiated), can be determined from measurements of the asymptotic value of $J(s)s^3$ and of Q using the relation

$$J(s)s^3(s \to \infty)/Q = S_v/16\pi^2\phi_1 \quad (7)$$

To calculate Q the SAXS curves are usually divided into two regions; the region of s lower than the value s_P at which Porod's law [12–14] begins to be satisfied and the region of higher s. In the first region Q was determined from the measured values of $J(s)$ and, for the second region, a contribution $J(s_P)s_P^2$ was added. This contribution takes into account extrapolated $J(s)$ values following Porod's law (Equation 5). The method is discussed fully elsewhere [7].

2.4. Other techniques and measurements

Thin foils for transmission electron microscopy (TEM) were prepared by ion beam thinning as described earlier [5].

Viscosity measurements were performed by the penetration method described in detail elsewhere [7, 15, 16]. The apparatus was calibrated using samples of NBS 710 and NBS 711 standard glasses.

3. Results and discussion

Part of the $BaO-SiO_2$ phase diagram of particular

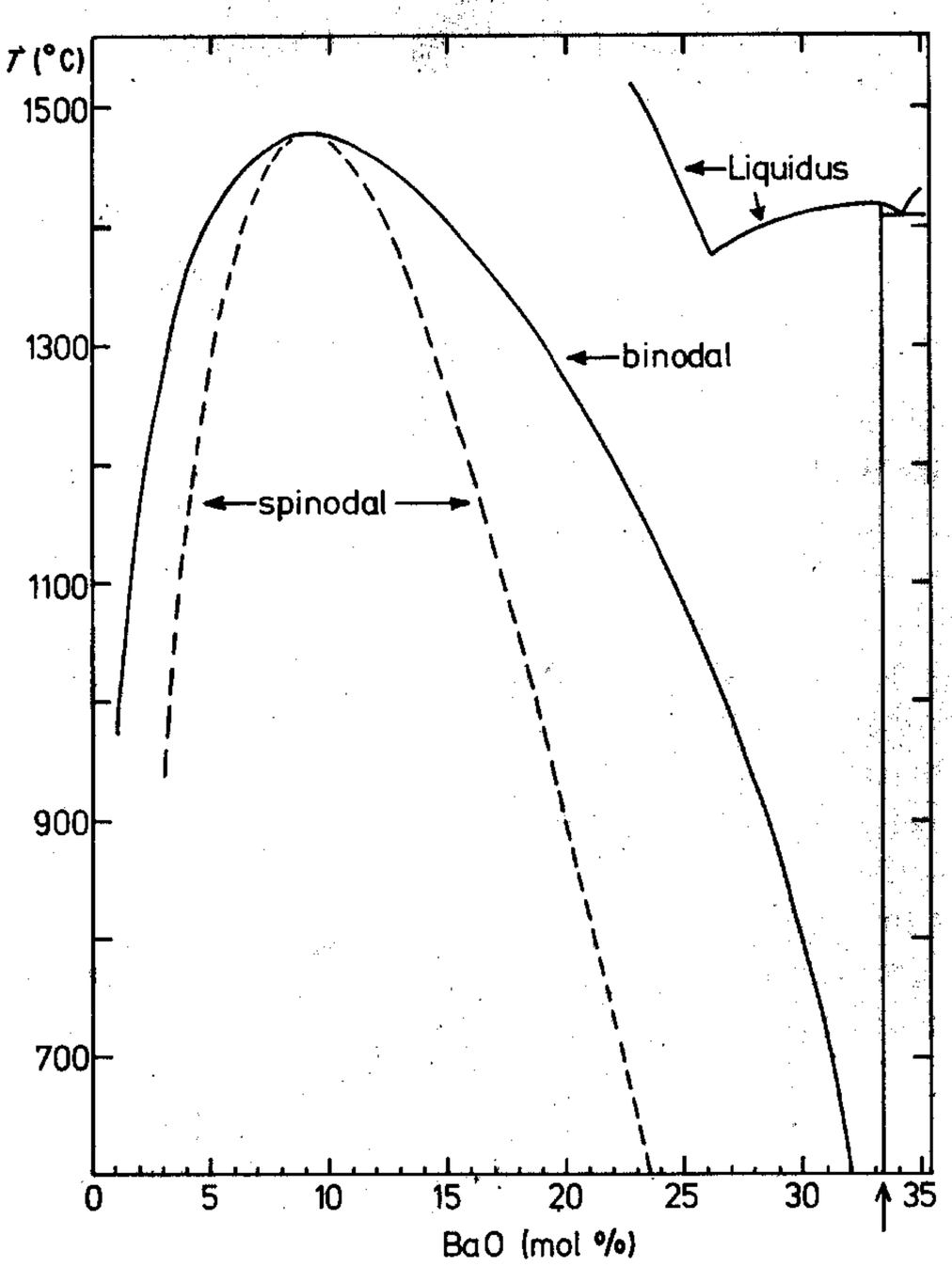

Figure 1 Part of the $BaO-SiO_2$ phase diagram. Sub-liquidus liquid–liquid immiscibility boundary (binodal) and spinodal curve from [17]. $BaO \cdot 2SiO_2$ composition indicated by ↑.

interest to the present study is shown in Fig. 1. The liquid–liquid immiscibility boundary (binodal) and spinodal curves are those given by Haller *et al.* [17].

3.1. Preliminary observations using electron microscopy

A detailed TEM study of the early stages of crystallization was made in Part 1. Here TEM of thin glass sections was used to look for the presence or absence of phase separation, to measure particle sizes for comparison with SAXS and to examine crystallization in the phase-separated glasses. These observations are important to the later sections.

As-quenched and non-heat treated specimens of glass 28.3 showed no detectable phase separation (Fig. 2a). Spherical silica-rich droplets were observed in glass 28.3 after heat treating at 743° C, their sizes increasing with time (Fig. 2b). The droplets were lighter in contrast than the surrounding baria-rich matrix phase. Droplets were also clearly observed after heating glass 28.3 at 760° C, their sizes again increasing with time (Fig. 2c, d). Fine-scale phase separation was also observed in glass 27.0 when heated at 743° C. When glass 28.3 was heated at 821° C for 22 min (to give the glass designated 28.3 BPS) the droplets were much larger (~40 nm diameter) while the number density was lower than for the treatments at 743 and 760° C (Fig. 2e). This specimen had a slight blue opalescence while samples heat treated at 743° C were visibly clear and transparent.

No phase separation could be detected by TEM in glass 29.7 H (Fig. 3a) even after heating for 5.5 h at 743° C followed by 4.2 h at 690° C and finally 1 h at 750° C. Specimens of this glass heated for 23 h at 710° C or for 48 h at 718° C were also free of phase separation.

These results appear to indicate that glass 29.7 H does not phase separate even when heated just inside the immiscibility gap since the nominal immiscibility temperature, T_m, for the glass calculated from the empirical equation of Haller *et al.* [17] is about 780° C (for the purposes of calculation the levels of BaO and SrO impurity were added together). A possible explanation is that the thermodynamic driving force was so small at temperatures between T_g (about 690° C) and T_m that phase separation was extremely slow and not observed. Such an effect was reported by Burnett and Douglas [18] in the soda–lime–silica system. Ramsden and James [5] also observed no trace of immiscibility in a 30.4 mol % BaO glass when heated just inside the nominal immiscibility gap.

It should be pointed out that the equation of Haller *et al.* was fitted to the T_m data of Steward *et al.* [19]. Although these data were only obtained in the higher temperature range (above 1000° C) the use of the equation at lower temperatures may be assumed to be reasonably accurate. Results obtained in Part 1 were in reasonable agreement with the equation.

The above explanation for the absence of phase separation in glass 29.7 H does not exclude the possibility of phase separation occurring if lower temperatures (higher undercoolings) are employed. The important point here is that no phase separation was detected in glass 29.7 H by TEM for the temperatures used in the present study. The same applied to the glass 29.9.

It should be noted that the kinetics of phase separation occur more rapidly as the silica content of the base glass is increased. This was shown by the electron microscope results in Part 1 and will also be demonstrated by the SAXS results (Section 3.3). Thus from SAXS the attainment of the equilibrium composition of the baria-rich matrix is much faster for glass 27.0 (72.6 mol % SiO_2) than for glass 28.3 B (71.3 mol % SiO_2).

When the phase-separated glass 28.3 BPS was given a further heat treatment of 743° C for 6 h there was no evidence from TEM for a secondary fine-scale droplet phase separation in the matrix phase. This is consistent with the previous discussion concerning the absence of phase separation in glass 29.7 H. In the case of glass 28.3 BPS the initial treatment at 821° C caused the baria-rich matrix to shift to approximately 29.8 mol % BaO (the immiscibility boundary), rendering nucleation of secondary droplets in the amorphous matrix difficult.

In agreement with the TEM study in Part 1, barium disilicate crystalline spheres and needles were observed in thin sections of samples subjected to long heat treatments. The needles appeared to grow through the amorphous baria-rich matrix in the phase-separated glasses, leaving the silica-rich droplets undisturbed. This is shown for glass 28.3 B heated at 743° C for 30.2 h in Fig. 3b. Also, the fine-scale phase separation appeared to have little influence on the morphology of the growing crystals. For comparison glass 29.9

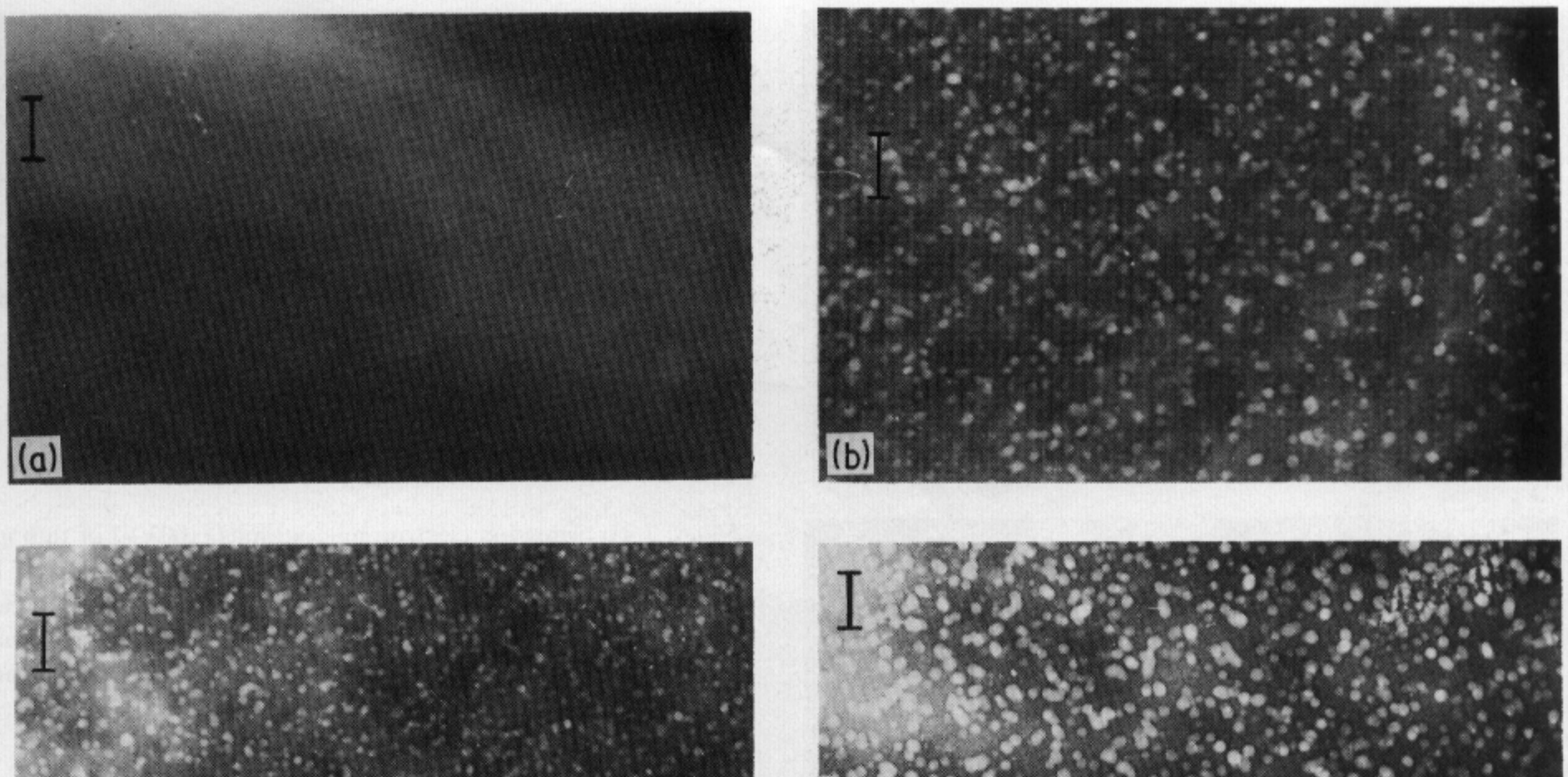

Figure 2 Transmission electron micrographs (100 kV) of thin glass sections of glass 28.3 B (28.3 mol % BaO). The bars denote 0.1 μm. (a) As-prepared (quenched) glass; (b) 743° C for 14.4 h; (c) 760° C for 3.7 h; (d) 760° C for 8.4 h; (e) 821° C for 22 min; (glass "28.3 BPS").

heated at 752° C for 13.1 h is shown in Fig. 3c. Here crystalline needles grew in a glass in which no amorphous phase separation was observed.

3.2. Crystal nucleation kinetics of barium disilicate: results

Samples of the glasses were given nucleation heat treatments at temperatures from 718 to 760° C and subsequent development (growth) treatments at 810 to 830° C for 10 to 30 min. In Fig. 4 crystal nucleation density (N_v) against time curves are plotted for glasses 28.3 A and 29.7 H at a nucleation temperature of 718° C. The most striking observations are that the nucleation rate I ($=dN_v/dt$) is constant for glass 29.7 H but increases continuously with time for glass 28.3 A. In fact no amorphous phase separation was observed in 29.7 H (Section 3.1) whereas phase separation occurred simultaneously with crystal nucleation in 28.3 A at 718° C.

Fig. 5 shows similar behaviour for the glasses after heat treatment at a nucleation temperature of 745° C. The nucleation rate of glass 28.3 A increases with time in the first few hours of treatment, reaching a constant value at longer times. The nucleation density (N_v) in glass 28.3 A is less than in glass 29.7 H at short times but exceeds that of 29.7 H after about 9 h. The maximum nucleation rate dN_v/dt of glass 28.3 A is much lower than in the stoichiometric barium disilicate glass 33.3 A (about 20 times lower), which is outside the immiscibility region. Only one point for glass 33.3 A is shown for comparison in Fig. 5. Detailed results for this glass are given in another paper [8]. The high nucleation rates in barium disilicate glass were also reported in Part 1 [5].

Glasses 28.3 A and 29.7 H were also nucleated at 760° C, and the N_v against time curves are shown in Fig. 6. The nucleation rate of glass 28.3 A is initially lower than that of 29.7 H, reaches a maximum value at about 2.5 h, overcoming the constant rate of 29.7 H, and levels off after 3 h, approaching a constant value. Even at this stage, dN_v/dt for glass 28.3 A is higher than the steady state rate of glass 29.7 H. With the exception of the inflexion, which gives a maximum value for dN_v/dt of glass 28.3 A at 760° C, the general behaviour is similar at 718, 745 and 760° C.

In order to check the reproducibility of the experimental data, and to test the possibility that the observed inflexion in the nucleation curve of glass 28.3 A was caused by the "development" heat treatment, a further "growth" treatment of 8 min at 815° C was given to the same specimens used previously. The new values of N_v are compared with the old ones in Fig. 7. The agreement is excellent. The origin of the inflexion will be discussed later.

Fig. 8 shows the nucleation curve for glass 28.3 B

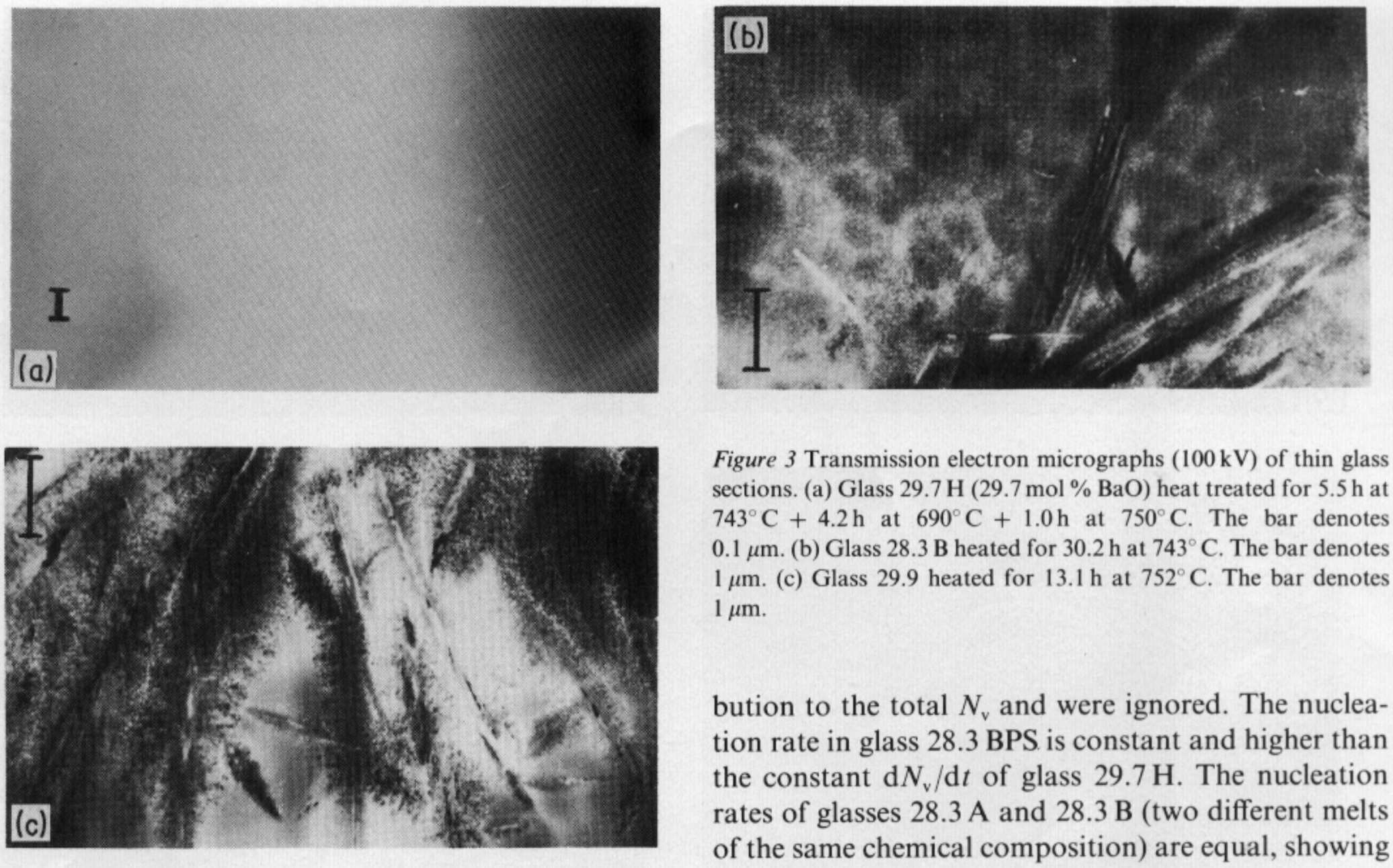

Figure 3 Transmission electron micrographs (100 kV) of thin glass sections. (a) Glass 29.7 H (29.7 mol % BaO) heat treated for 5.5 h at 743° C + 4.2 h at 690° C + 1.0 h at 750° C. The bar denotes 0.1 μm. (b) Glass 28.3 B heated for 30.2 h at 743° C. The bar denotes 1 μm. (c) Glass 29.9 heated for 13.1 h at 752° C. The bar denotes 1 μm.

first heat-treated at 821° C for 22 min to cause a pronounced development of the amorphous phase separation. The blueish appearance of the glass samples and the rather large size of the silica-rich droplets (Fig. 2e) after this treatment was an indication that the amorphous phase separation had reached an advanced stage. These specimens will be referred to as 28.3 BPS. Then, the same specimens were subjected to the common standard double-stage crystal nucleation and growth heat-treatment at 743 and 820° C. A few crystals, much larger than the average size, could be seen in the micrographs. These were formed during the first heat treatment. They made a negligible contribution to the total N_v and were ignored. The nucleation rate in glass 28.3 BPS is constant and higher than the constant dN_v/dt of glass 29.7 H. The nucleation rates of glasses 28.3 A and 28.3 B (two different melts of the same chemical composition) are equal, showing the reproducibility of the present experiments, and increase continuously up to about 7 h, when they approach a constant value which is higher than dN_v/dt for glasses 28.3 BPS and 29.7 H.

The nucleation curve of glass 27.0 heated at 743° C is shown in Fig. 9 together with the curve for glasses 28.3 A and 28.3 B. The nucleation rate of glass 27.0 increases up to about 2 h, which is much shorter than the 7 h period required for glasses 28.3 A and 28.3 B to reach a constant equilibrium rate. After these periods, the crystal nucleation rates of the glasses are constant and equal.

Fig. 10 shows the crystal nucleation density (N_v) against time curves for glasses 27.0, 28.3 B and 29.9 nucleated at 752° C. The dN_v/dt of glass 28.3 B increases up to about 3 h. It then appears to pass through a maximum, decreases and becomes constant

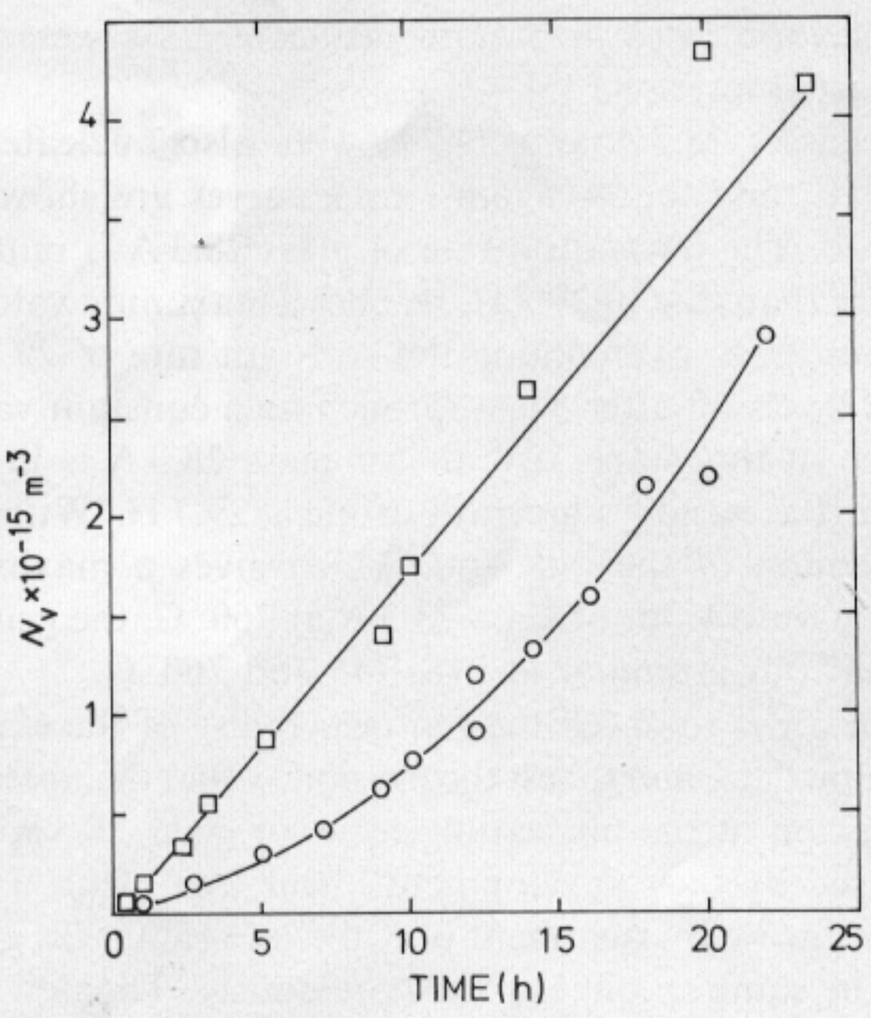

Figure 4 N_v against time (t) plots for glasses (○) 28.3 A and (□) 29.7 H at nucleation temperature of 718° C (N_v is the number of internally nucleated crystal spherulites of barium disilicate per unit volume).

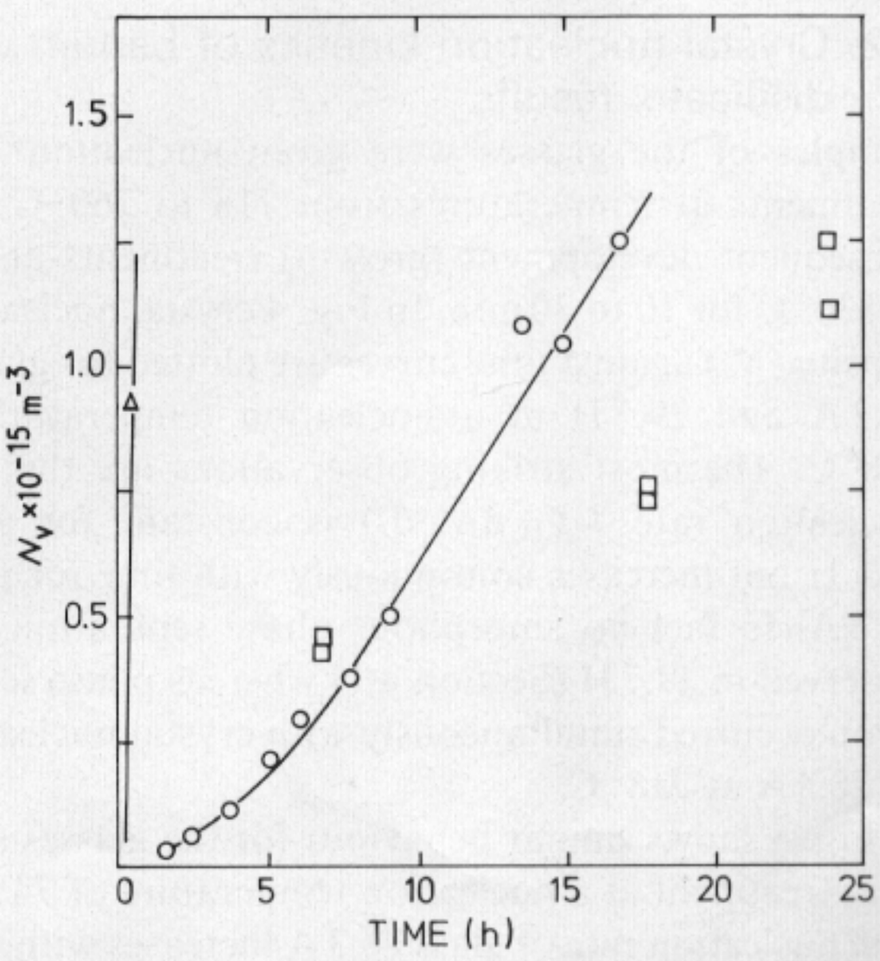

Figure 5 N_v against time for glasses (○) 28.3 A, (□) 29.7 H and (△) 33.3 A at nucleation temperature of 745° C.

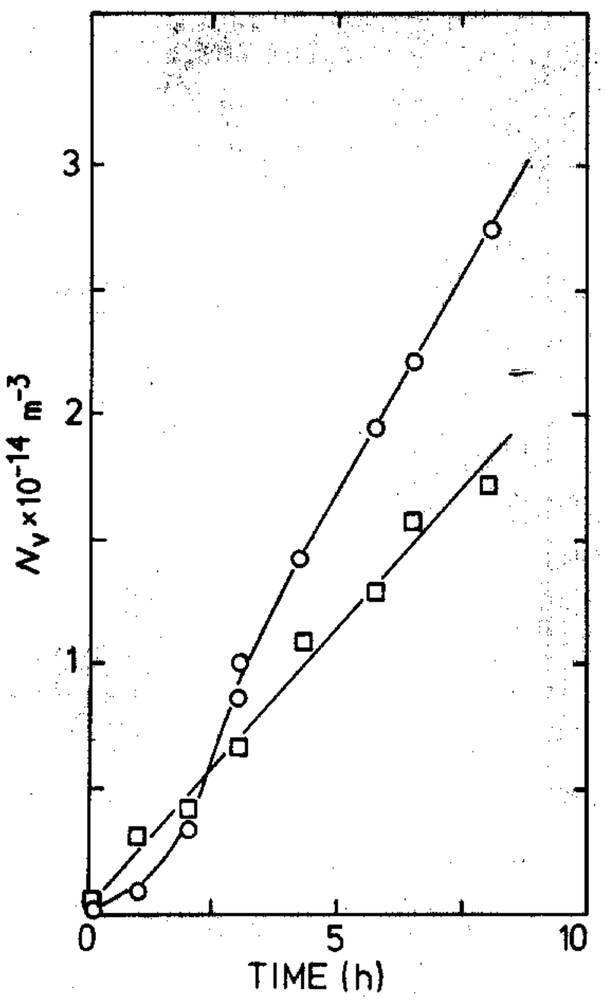

Figure 6 N_v against time for glasses (○) 28.3 A and (□) 29.7 H at nucleation temperature of 760° C.

after about 5 h heat treatment. The nucleation rate of glass 27.0 increases up to about 2 h, when it approaches a constant value equal to the nucleation rate of glass 28.3 B, and slightly higher than the constant rate of glass 29.9.

It is clear that the crystal nucleation rates of glasses 27.0, 28.3 A and 28.3 B, which are undergoing amorphous phase separation, increase with time, in some cases passing through a maximum, and approach a constant value. The nucleation rates of glasses 29.7 H and 29.9, which do not phase separation (Section 3.1) are constant from the beginning, being higher than dN_v/dt of the phase separating glasses only in the initial parts of the nucleation curves (for short nucleation treatments).

3.3. Kinetics of amorphous phase separation; small-angle X-ray scattering results

The kinetics of amorphous phase separation were studied by SAXS in glass 27.0 after heating at 743° C from 0 to 17 h, and in glass 28.3 B after heating at 743° C from 0 to 30 h and at 760° C from 0 to 8 h. The

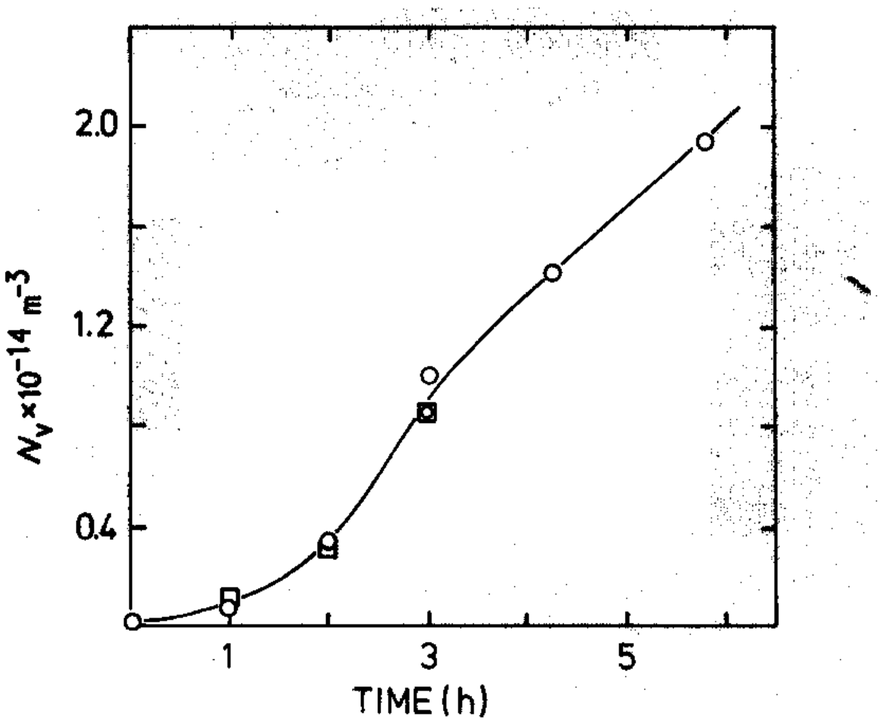

Figure 7 N_v against time for glass 28.3 A at nucleation temperature of 760° C subjected to two different development heat treatments ((○) 26 min at 820° C, (□) 26 min at 820° C + 8 min at 815° C).

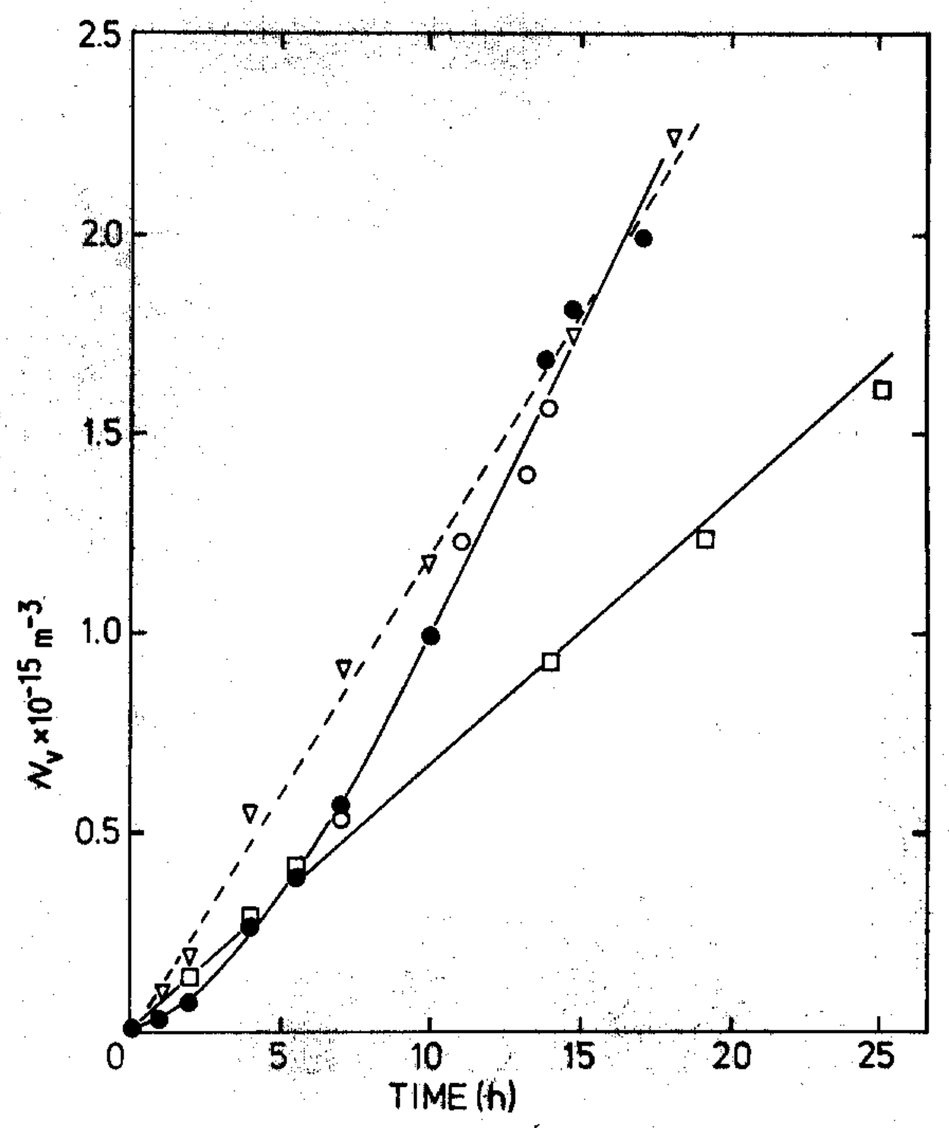

Figure 8 N_v against time for glasses (○) 28.3 A (●) 28.3 B, (▽) 28.3BPS and (□) 29.7 H at nucleation temperature of 743° C. (---) glass 28.3 BPS (previously phase separated at 821° C for 22 min prior to nucleation at 760° C and development at 820° C).

experimental SAXS intensities, J, are given as functions of the scattering angle, ε, instead of the modulus of the scattering vector, s, used in section 2.3 ($s = \varepsilon/\lambda$, λ being 0.154 nm in this work). A typical set of normalized intensity curves of J against ε in arbitrary units for glass 27.0 at 743° C are shown in Fig. 11. The curves for glass 28.3 B at 743° C and at 760° C were similar. All the curves, except those for very short heat treatments show a maximum at small ε, which is associated with interference in the X-ray scattering between particles. This phenomenon is expected when the volume fraction of particles exceeds 1 or 2%, a condition applying in the present case since the

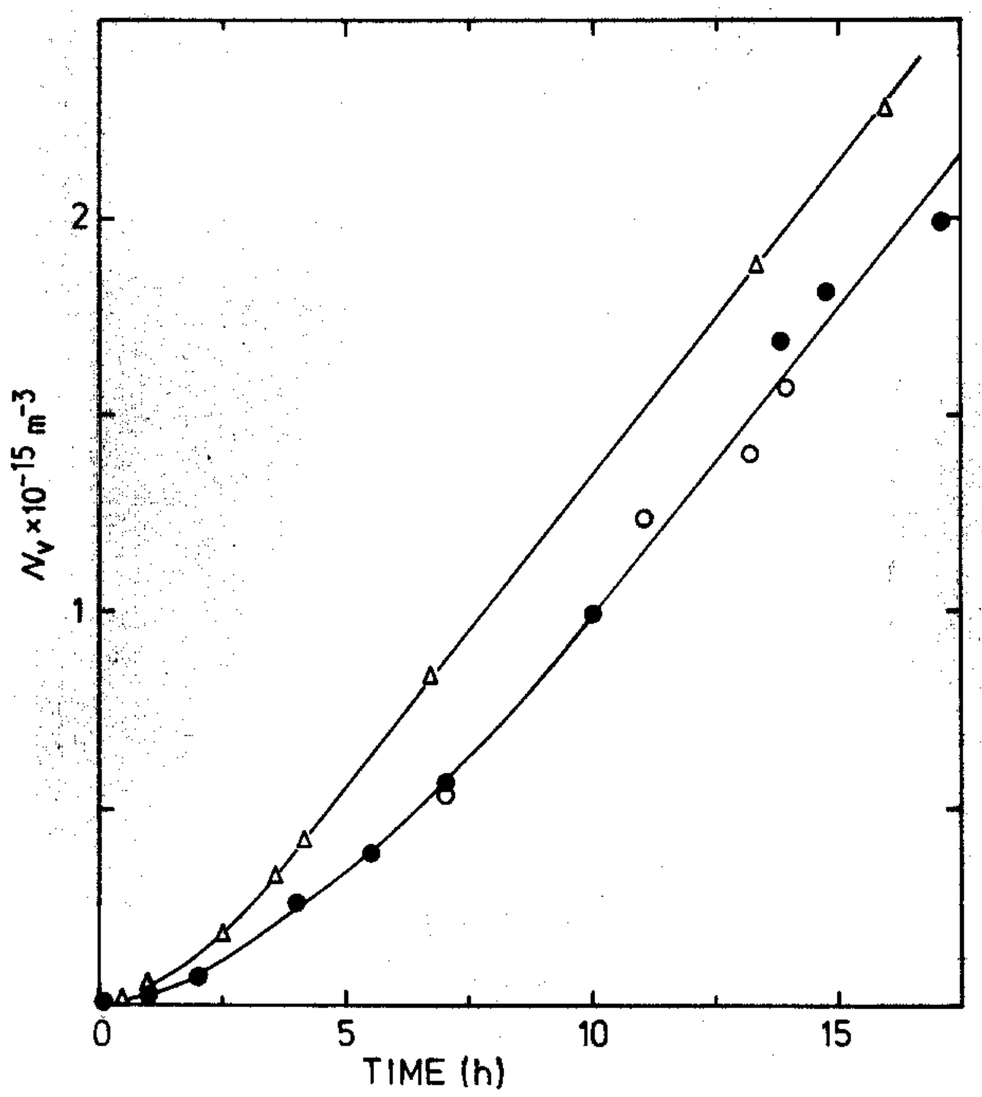

Figure 9 N_v against time for glasses (△) 27.0, (○) 28.3 A and (●) 28.3 B at nucleation temperature of 743° C.

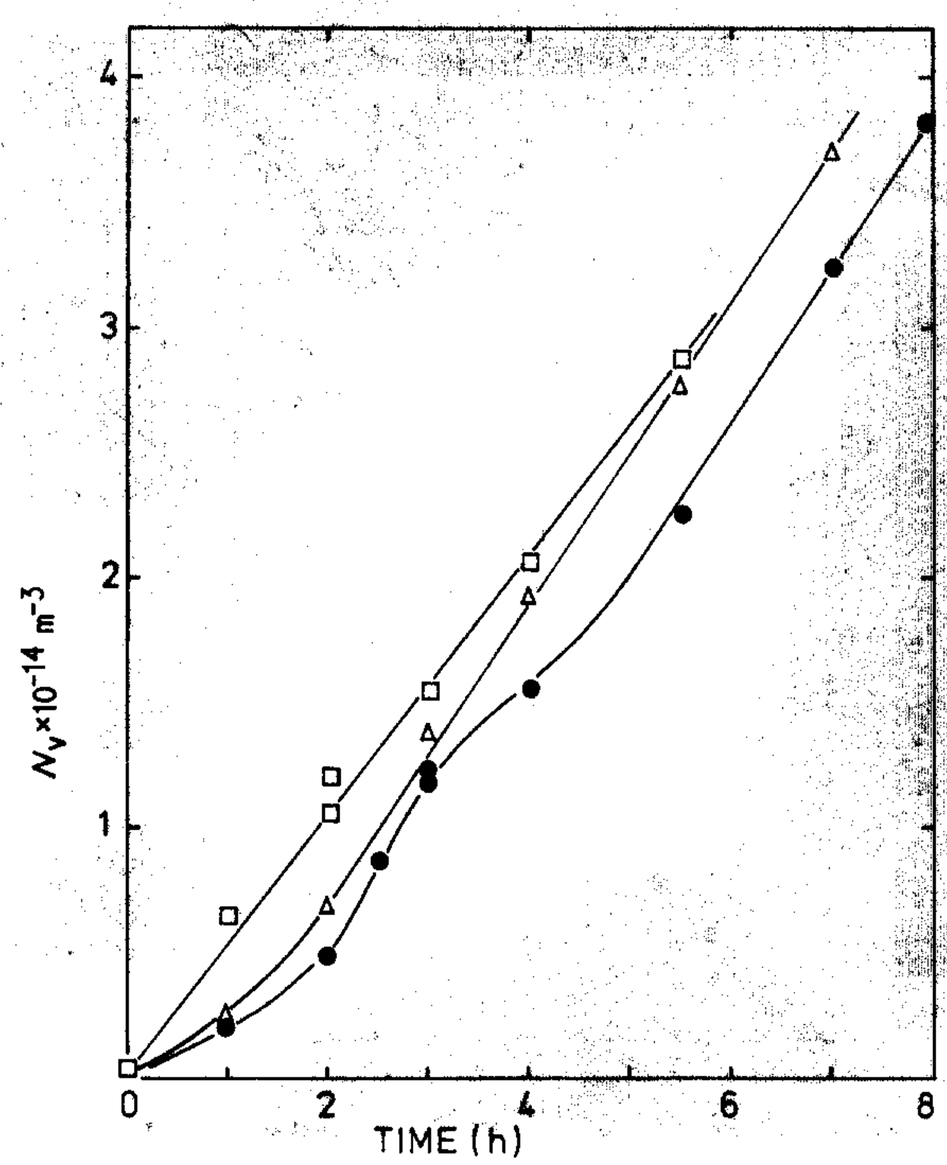

Figure 10 N_v against time for glasses (△) 27.0, (●) 28.3 B and (□) 29.9 at nucleation temperature of 725° C.

equilibrium volume fractions of the silica-rich particles calculated from the binodal boundary were 0.19, 0.15 and 0.11 for glass 27.0 at 743° C, glass 28.3 B at 743° C and glass 28.3 B at 760° C, respectively.

Guinier plots of log J against ε^2 were obtained. Two sets of results are shown in Figs 12 and 13. The plots were linear over a large angular range indicating narrow size distributions similar to the observations of Neilson [20] and Gerold [21] for other glasses and metallic alloys. The average diameters, D, of the scattering particles were determined from the slopes of the Guinier plots using Equation 1. Plots of log D against log (time) are given in Fig. 14.

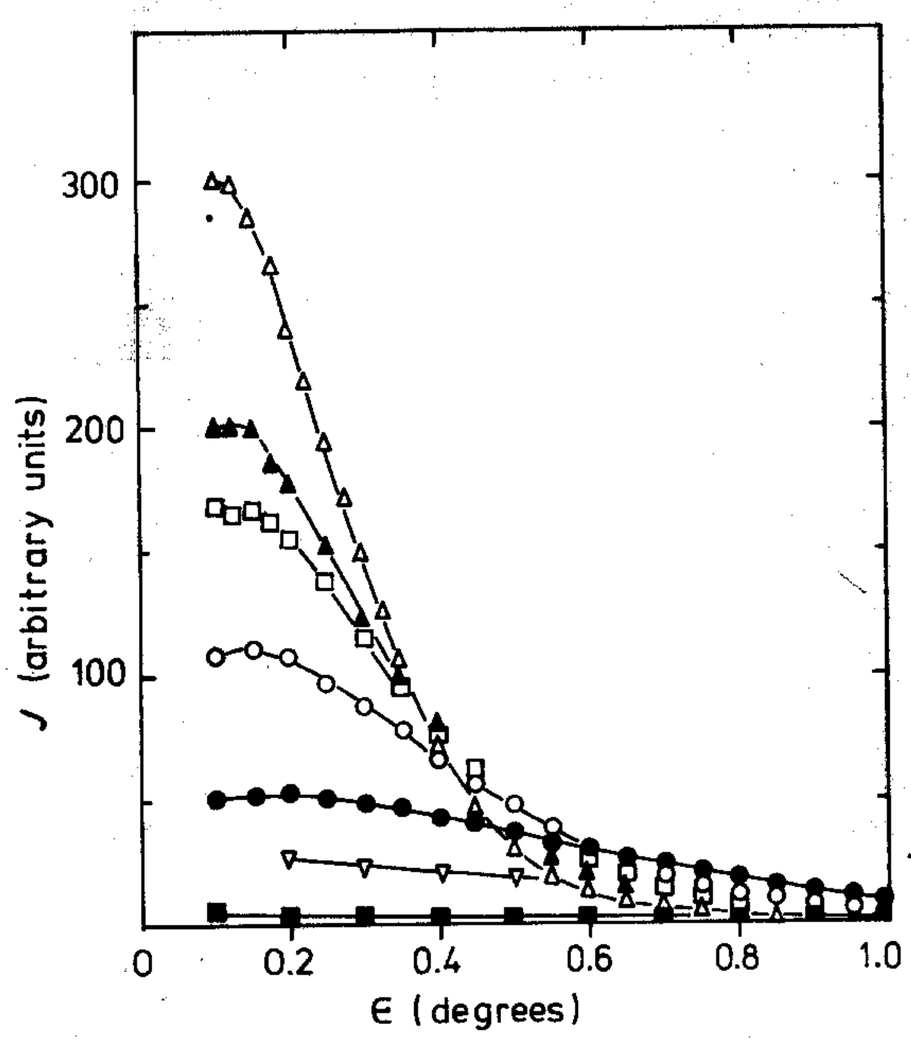

Figure 11 SAXS curves of measured, normalized, intensity, J, against scattering angle, ε, for glass 27.0 heat treated at 743° C for (■) 0 h, (▽) 0.5 h, (●) 2.5 h, (○) 6.7 h, (□) 9.3 h, (▲) 13.3 h, (△) 17 h.

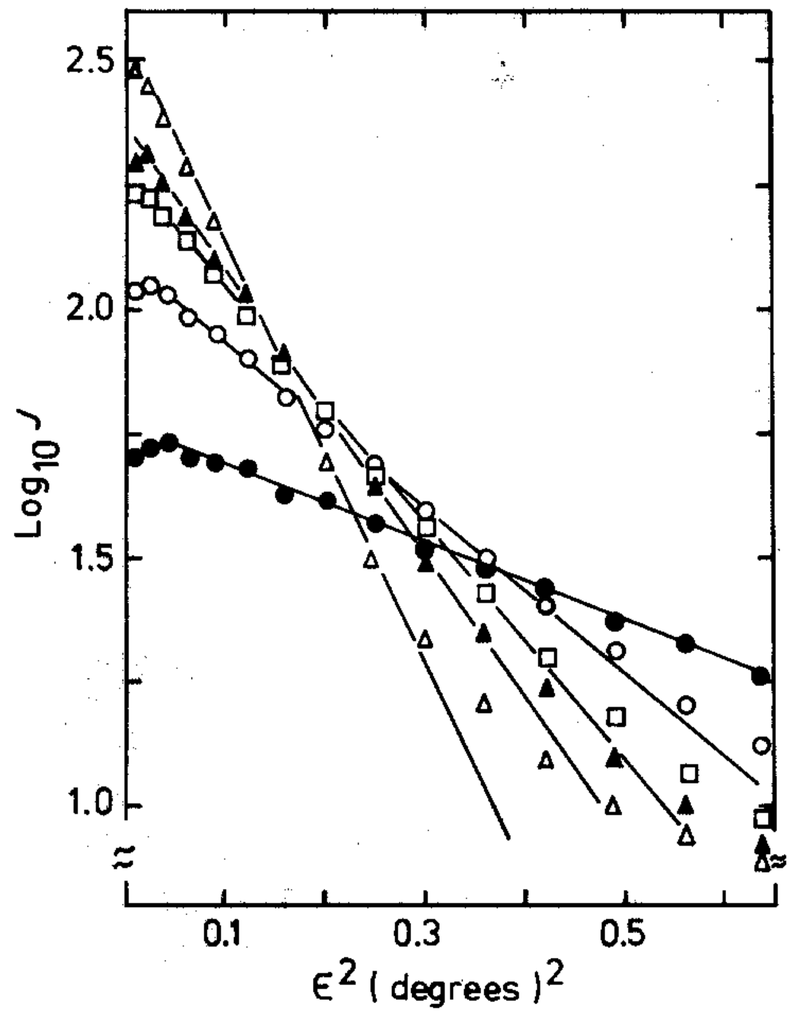

Figure 12 Guinier plots ($\log_{10} J$ against ε^2) of SAXS results for glass 27.0 heat treated at 743° C for (●) 2.5 h, (○) 6.7 h, (□) 9.3 h, (▲) 13.3 h, (△) 17.0 h.

The average diameters from SAXS and from TEM of thin glass films were in reasonable agreement (Fig. 14), although the TEM values tended to be somewhat higher, particularly at earlier times. The discrepancy can be attributed at least partially to errors in the TEM values because of particle overlapping. Also the average diameter determined from the Guinier plots is expected to be less than the real average diameter for a concentrated system of particles [22]. In the latter case, the magnitude of the underestimation depends on the volume fraction of the particles, which is constant after the matrix reaches its equilibrium composition.

The slopes of the plots in Fig. 14 for glass 28.3 B heat treated at 760 and 743° C are close to $\frac{1}{3}$. This is in agreement with the theory of diffusion controlled Ostwald ripening which predicts a $D \propto t^{1/3}$ relationship (where t is the time) [3] in the later stages when the

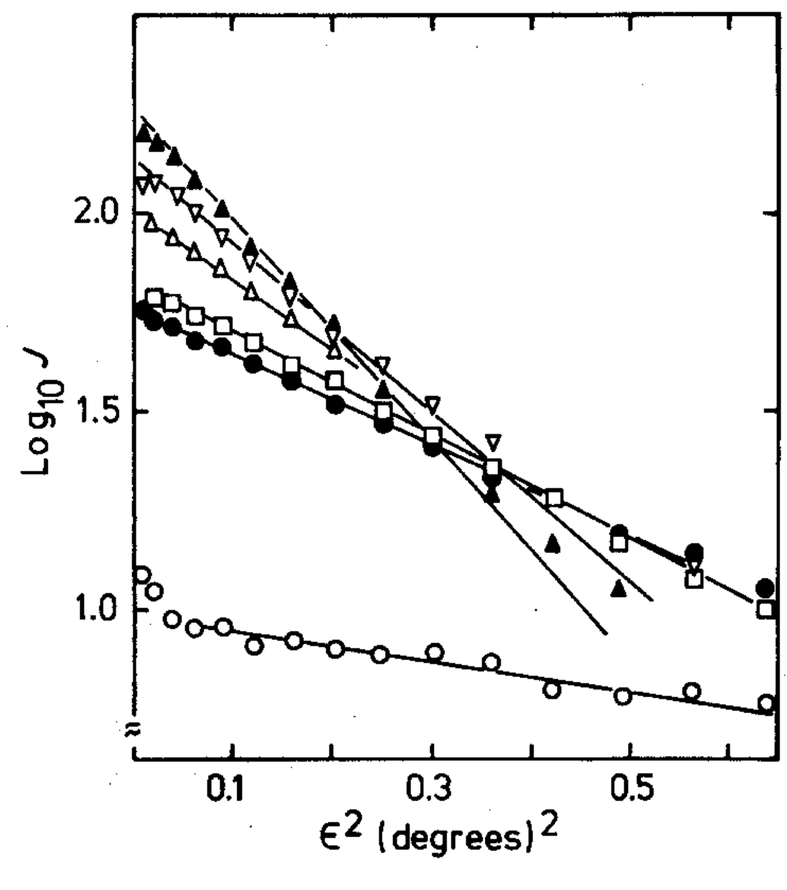

Figure 13 Guinier plots ($\log_{10} J$ against ε^2) of SAXS results for glass 28.3 B heat treated at 743° C for (○) 1 h, (●) 3 h, (□) 5 h, (△) 7 h, (▽) 10 h, (▲) 14 h.

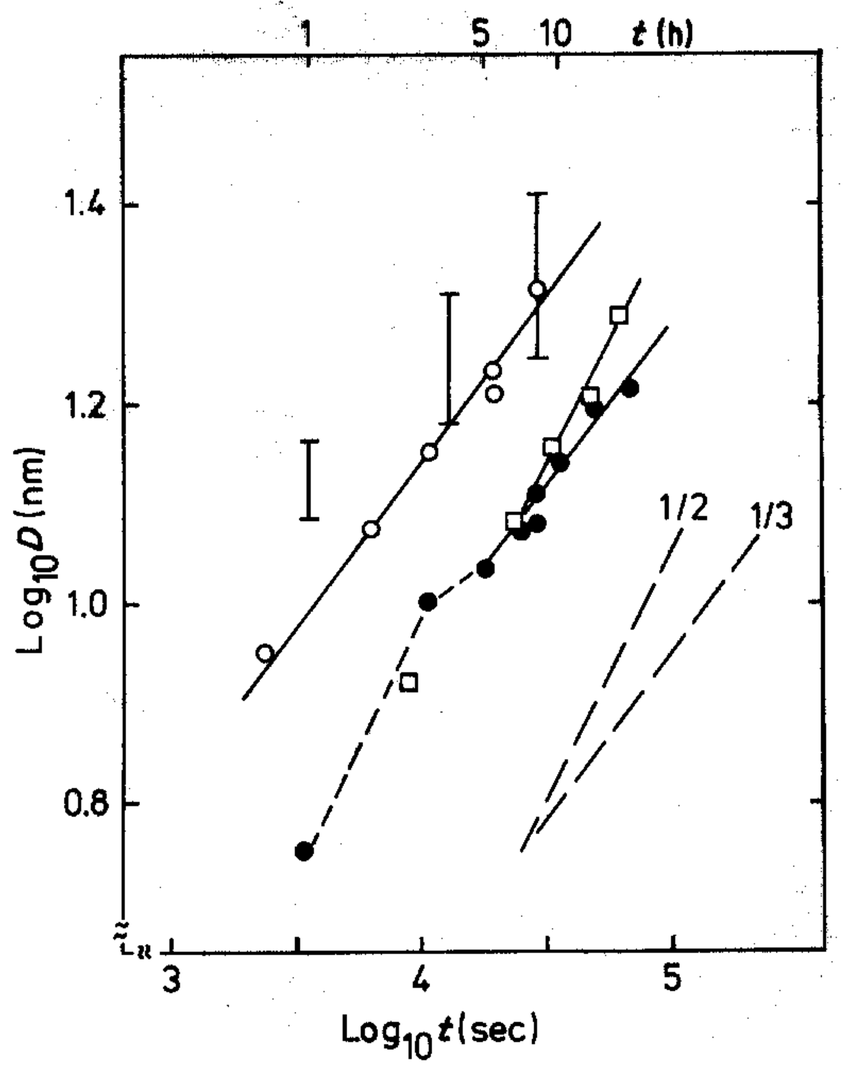

Figure 14 $Log_{10}D$ against $log_{10}t$ plots for (□) glass 27.0 at 743° C, (●) glass 28.3 B at 743° C and (○) 28.3 B at 760° C. D is the average diameter from Guinier plots, t the time of heat treatment. TEM values for glass 28.3 B at 760° C indicated by vertical bars.

volume fraction of precipitated phase is approaching its equilibrium value. In the early stages when nucleation and growth predominate, a $D \propto t^{1/2}$ relationship is expected. For glass 27.0 at 743° C the plot in Fig. 14 has a slope apparently greater than $\frac{1}{3}$. However, this is tentative in view of the small number of experimental points. Also this apparent behaviour cannot be explained by nucleation and growth since the phase separation is not in the early nucleation and growth stage as will be shown later. It should also be noted that the slope in Fig. 14 for glass 28.3 B at 743° C is also possibly greater than $\frac{1}{3}$ for the shortest times, although this is again tentative.

The evolution of Q, the integrated SAXS intensity, with time of isothermal treatment is shown in Fig. 15. It can be seen that Q initially increases with time but eventually approaches a constant value corresponding to the two phases attaining their equilibrium compositions. The constant value of Q is approached after 3 to 4 h at 760° C and after 7 h at 743° C for glass 28.3 B. For glass 27.0 at 743° C, Q is constant from a time of less than 2.5 h heat treatment, indicating very rapid phase separation in this glass. The increase in Q observed for glass 28.3 B heated at 743° C for 30.2 h is probably associated with a high degree of crystallization in this sample, as shown by TEM. A similar observation has been made in Li_2O-SiO_2 glasses [23]. The maximum error in the Q values was about 10%.

From the SAXS curves further information was obtained including the number of particles per unit volume, n_v (in relative units), the interfacial area per unit volume S_v, and the average volume of the particles v. These results will be summarized since they are relevant to the present study. However, only an outline of the calculations will be included (for further details see [7, 24]).

It can be shown that the number of droplets n_v (in relative units) is given by $KJ(0)/\Delta\varrho^2 D^5$ where $J(0)$ is

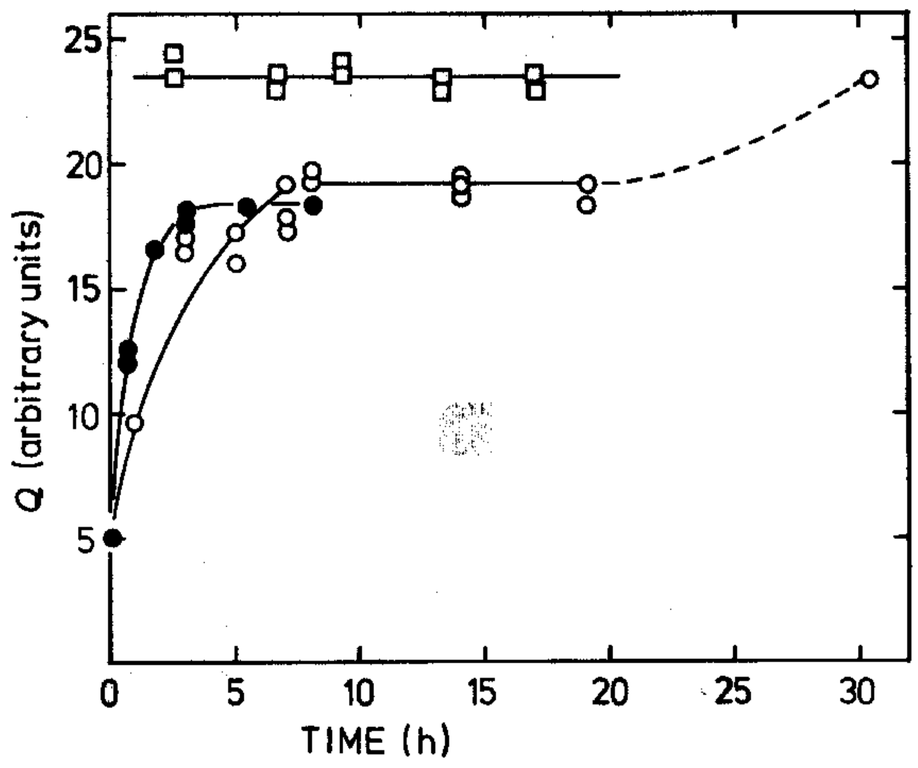

Figure 15 Integrated SAXS intensity Q for $BaO-SiO_2$ glasses heat treated at 743 and 760° C, against time (t) of heat treatment. (□) Glass 27.0 at 743° C, (○) glass 28.3 B at 743° C, (●) glass 28.3 B at 760° C.

the measured intensity at $s = 0$ for an "infinitely high beam" of negligible width and is determined from the Guinier plots (Equation 1); and K is a constant. If we assume $\Delta\varrho$ is constant the variation of n_v with time of isothermal treatment may be followed. The values are listed in Table II. It should be stressed that the n_v values for different glasses, or the same glass heated at different temperatures are not directly comparable because $\Delta\varrho^2$ is not the same in each case. When plots of n_v against $1/t$ (not shown here) are made straight lines fit the data reasonably well for glass 27.0 at 743° C and 28.3 B at 760° C, as expected for diffusion-controlled Ostwald ripening. However, for glass 28.3 B at 743° C there is a change in slope after 8 h when n_v begins to decrease more rapidly. It should be noted (Table II) that n_v decreases from the earliest times studied, indicating that in these samples most of the nucleation of droplets occurs either during cooling from the melt or within a very short time of heat treatment. The particles appear to dissolve more rapidly, however, when the matrix reaches its equilibrium composition (compare Table II and Fig. 15 for glass 28.3 B at 743° C). Also it should be remarked that the early period of slower decrease in n_v for 28.3 B at 743° C coincides with the (tentative) $t^{1/2}$ variation of droplet diameter. These observations are of particular interest since they show that the coarsening stage begins well before the attainment of the equilibrium matrix composition which is given by a constant value of Q. A similar result was found by Kirkwood [25] for the coarsening of precipitates in metallic alloys.

The interfacial areas, S_v, determined from Porod's law (see Equation 2 and [24]) and by using an alternative method due to Debye *et al.* [26] are given in Table II. The two sets of values are in reasonable agreement, the Porod values being somewhat lower than the Debye values. S_v decreases with time as expected for the coarsening stage of phase separation.

It is also possible to determine the average volume, v, of the particles from measurements of $J(0)$ and Q. The details of the method are given in [7]. The values of the average diameter D_1 obtained from v using $D_1 = (6v/\pi)^{1/3}$ were slightly smaller than the values of

TABLE II Structural parameters determined from SAXS

Time (h)	n_v (relative units)	S_v ($mm^2\,mm^{-3} \times 10^{-4}$)		v ($nm^3 \times 10^{-3}$)
		Debye	Porod	
27.0 743° C ($\phi_1 \simeq 0.19$)				
2.5	1.460	41.4	24.3	0.200
6.67	0.480	18.2	15.8	0.632
9.33	0.287	16.3	11.3	1.113
13.33	0.202	16.0	10.4	1.556
17	0.124	14.5	8.0	2.856
28.3 B 743° C ($\phi_1 \simeq 0.15$)				
1	1.700	–	–	–
3	0.534	25.8	15.9	0.055
5	0.455	25.5	13.6	0.342
7	0.405	21.8	12.7	0.417
8	0.380	–	13.4	0.585
10	0.270	17.7	10.7	0.880
14	0.175	15.4	9.2	1.431
19	0.144	–	9.2	1.471
30.2	0.063	–	5.5	4.80
28.3 B 760° C ($\phi_1 \simeq 0.11$)				
0.67	0.550	22.3	13.8	0.237
1.75	0.347	16.6	9.5	0.572
3	0.227	13.0	7.9	1.001
5.4	0.161	11.8	6.2	1.587
8	0.084	8.6	3.7	3.464

the Guinier diameter, D, the ratio D_1/D being nearly constant at about 0.88. This indicates [7] that the particle size distribution is narrow and the magnitude of the departure from a monodispersed system changes very little with time of heat treatment. It can also be concluded that the shape of the size distribution is similar for glass 27.0 heated at 743° C and for glass 28.3 B heated at 743 and 760° C.

3.4. The effects of amorphous phase separation on crystal nucleation kinetics

We are now in a position to correlate the results of the crystal nucleation studies (Section 3.2) with the data on the kinetics of amorphous phase separation in the same glasses (Section 3.3). It was shown that the crystal nucleation rates for the phase separating glasses 27.0, 28.3 A and 28.3 B, increase with time in the early stages, approaching constant values for longer times. The time to reach a constant rate decreases with increasing temperature. In contrast, nucleation density plots for the non-phase separating glasses, 29.7 H and 29.9, are straight lines from the beginning. From Fig. 9, it is clear that the crystal nucleation rates in glasses 27.0 and 28.3, heated at 743° C, increase for times up to 2 and 7 h, respectively. After these periods they remain constant and equal for the two glasses. The integrated SAXS intensity at 743° C (Fig. 15) also increases up to $t < 2.5$ h for glass 27.0 and up to 7 h for glass 28.3 B, remaining unchanged after these periods. As discussed previously, the increase in Q indicates that the composition of the amorphous matrix is changing with time until equilibrium is approached (constant value of Q). Therefore, this is strong experimental evidence that the increase in crystal nucleation rates results from the compositional shift of the amorphous matrix (enrichment in BaO) brought about by phase separation. This conclusion is further supported by the curves of Figs 6 and 15 for the glass with 28.3 mol % BaO at 760° C which show that both the nucleation rate of crystals and the integrated intensity increase for times up to about 3 h.

The fact that the "equilibrium" crystal nucleation rates, I, in glasses 27.0 and 28.3 B at longer times, are equal at two temperatures (Figs 9 and 10), implies that I is only a function of the chemical composition of the phase separated matrix and does not depend on the volume fraction of the amorphous droplets. This statement becomes clearer if we refer to the miscibility gap shown in Fig. 1. For a given glass, the composition of the amorphous phase (binodal line) is only a function of temperature, being therefore equal for glasses 27.0 and 28.3 B when phase separated at the same temperature. On the other hand, the volume fraction of droplets given by the lever rule, is larger for glass 27.0 than for glass 28.3 B.

Fig. 8 shows that the crystal nucleation rate in glass 28.3 BPS, which was fully phase separated at 821° C before the nucleation treatment at 743° C, is constant from the beginning, and initially is higher than the nucleation rate of the as-quenched glass 28.3 B, for which phase separation proceeded simultaneously with crystal nucleation. When the matrix reached its equilibrium composition in glass 28.3 B, i.e. after 7 h at 743° C (Fig. 15) its nucleation rate overtook that of glass 28.3 BPS. This arises from the shape of the immiscibility boundary, the BaO content in the amorphous matrix being lower at 821° C than at 743° C. It should be mentioned, however, that if secondary phase separation had occurred in glass 28.3 BPS when nucleated at 743° C, the composition of the matrix would be equal for both glasses. However, transmission electron micrographs show no evidence for secondary phase separation in this glass. A much longer time is probably required for further (secondary) phase separation to fully develop at 743° C.

At this point, the possible influence of the interfaces of the phase separated microstructure on the nucleation of crystals must be considered. According to the SAXS results the average size of the droplets increases and the number and specific surface area of the droplets decrease from the very beginning of heat treatment. Therefore, the number of crystals which could eventually nucleate at the interfaces between the amorphous phases, if any, should also decrease with time. However, a decrease in crystal nucleation rate was never observed.

Finally, the fact that the crystal nucleation rates in the phase separating glasses, 27.0, 28.3 A and 28.3 B, increase with time, overtaking the constant nucleation rates in the non-phase separating glasses, 29.7 H and 29.9, at 718, 743, 745, 752 and 760° C, reinforces the conclusion that the observed increase in crystal nucleation rates is caused by the enrichment in BaO (of the matrix) resulting from phase separation. After the completion of phase separation, the matrix in glasses 27.0, 28.3 A and 28.3 B have the same percentage of BaO, which is higher than the BaO contents in glasses 29.7 H and 29.9. Although the latter glasses were probably situated just inside the miscibility gap for the temperatures used they did not phase separate for the reasons discussed earlier.

These conclusions are in excellent agreement with the general conclusions of Ramsden and James in Parts 1 and 2 of the present paper, i.e. the morphology of the phase separation has, at most, a minor influence on crystal nucleation and the predominant reason for the effects observed is the progressive shift in composition of the matrix phase with time as a result of phase separation. It is interesting to note that similar behaviour has recently been observed in the Li_2O–SiO_2 system [27].

An additional, smaller effect to that of the compositional changes was observed in the nucleation curves obtained in the present work. Thus, an inflexion was clearly observed in the nucleation curve for glass 28.3 A nucleated at 760° C (Figs 6 and 7), corresponding to a maximum value in dN_v/dt higher than the constant nucleation rate achieved at longer times. An inflexion was also observed for glass 28.3 B nucleated at 752° C (Fig. 10). A similar effect may possibly just be discernible at 745 and 743° C (some points are higher than the "smooth" curves in Figs 5 and 9), but no inflexion can be seen at 718° C (Fig. 4). In all cases, the inflexion in N_v occurred before the attainment of the equilibrium composition by the baria-rich amorphous phase as given by a constant value of Q (Fig. 15). A similar effect was observed by Tomozawa [23] and Zanotto and Craievich [28] in phase-separating Li_2O–SiO_2 glasses. Their results were attributed to some additional heterogeneous nucleation in the diffusion zones which exist around the amorphous droplets when the amorphous phase separation is in the early stages. The fact that the maximum in the nucleation rate (inflexion in N_v) is more pronounced as the temperature increases (nucleation rates decrease) shows that this is a relatively minor effect, being masked when the homogeneous nucleation rates are high, i.e. for temperatures approaching T_g.

3.5. The effects of amorphous phase separation on viscosity measurements

The initial objective was to measure the viscosity of certain glasses during the development of amorphous phase separation. Such information would be useful in interpreting the crystal nucleation kinetics in these glasses. However, to obtain accurate data it was necessary to use relatively thick ($\geqslant 8$ mm) glass samples in the penetration apparatus [7, 16] and unfortunately it was virtually impossible to obtain such thick specimens free of extensive phase separation, the latter occurring during cooling from the melt. Therefore, thin glass specimens 1.60 to 1.75 mm thick and 12.0 mm diameter, were used. The viscosity values of a number of the glasses at 732.0 ± 0.5° C are plotted in Fig. 16. It should be stressed that there is a systematic error in these values due to the small sample thickness but it should be approximately constant for all samples. The temperature of 732° C was chosen with the requirements of a relatively slow development of the amorphous phase separation and a reasonable time for the viscosity measurements. However, it was necessary to leave the samples for 30 to 40 min in the viscometer furnace to achieve equilibrium, and the amorphous separation could have developed substantially during that time. Fig. 16 also shows that glass 28.3 B, heated for 1 and 5 h before the measurements, does not exhibit any appreciable variation in viscosity. Consequently, the only general conclusion which can be made is that glass 33.2 B has an appreciably lower viscosity than glasses 27.0, 28.3 B and 29.9, which have similar viscosities at this temperature. It should be emphasized, however, that the amorphous separation could have been quite well-developed in glasses 27.0 and 28.3 B before the measurement was completed.

More extensive viscosity data for a barium disilicate glass are reported elsewhere [8].

3.6. The effects of amorphous phase separation on crystal growth rates

Specimens of glasses 28.3 A and 29.7 H, which were nucleated for increasingly longer periods of time at 718, 745 and 760° C and then "developed" at a

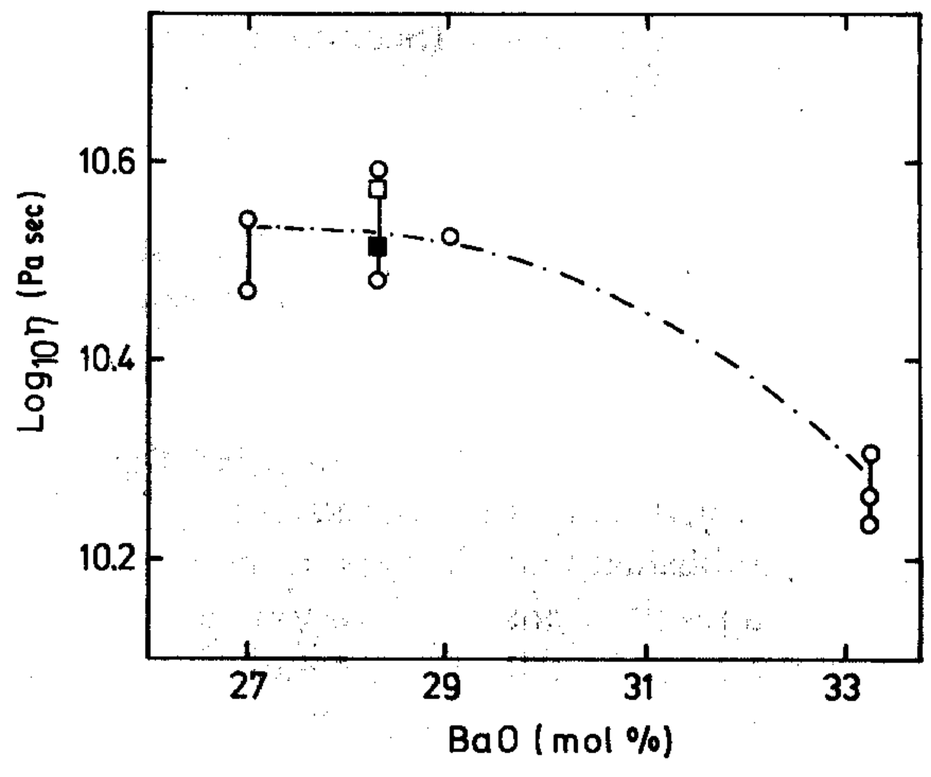

Figure 16 Viscosity, η, of BaO–SiO_2 glasses at 732 ± 0.5° C using thin specimens (see text), plotted against glass composition. (○) As-quenched glasses, (□) heat treated for 1 h at 743° C, (■) treated for 5 h at 743° C.

TABLE III Crystal growth rates in glasses 28.3 A, 29.7 H and 33.3 A ($m\,sec^{-1} \times 10^{10}$)

Glass	718° C	745° C	760° C
28.3 A	0.40	1.0	1.8
29.7 H	0.45	0.61	0.95
33.3 A	–	3.24	4.63

higher temperature (the same temperature and time of development being employed for each particular glass composition and nucleation temperature), show larger crystal diameters with increasing nucleation periods. Therefore, by measuring the maximum diameters of the spherulites shown in optical micrographs and assuming that: (i) the crystal growth rate is independent of size, and (ii) the "development" heat treatment brings an equal additional growth to each nucleus, it was possible to estimate the growth rates of the crystals in the nucleation range of temperatures. Plots of the maximum spherulites diameters against nucleation time at 718, 745 and 760° C for glasses 28.3 A and 29.7 H gave good straight lines and the growth rates increased with temperature (Table III). At 745 and 760° C the growth rates in glass 28.3 A were higher than in 29.7 H. At 718° C the growth rates in 28.3 A and in 29.7 H were about equal (Table III). Growth rates were also measured in the barium disilicate composition 33.3 A. In this case the largest crystalline needles (see [5]) were measured after a single stage heat treatment at 745 and 760° C. As expected the rates in 33.3 A were higher than in glasses 28.3 A or 29.7 H. The values are in close agreement with those for the 33.1 glass (B6) studied in Part 1 [5].

The observations for glasses 28.3 and 29.7 indicate that at 745 and 760° C phase separation has the effect of increasing the growth rate of glass 28.3 A so that it is greater than the growth rate of the non-phase separating glass 29.7 H, although the overall composition of the latter is higher in BaO. This can be explained by a similar argument to that used in discussing the nucleation kinetics. Thus in 28.3 A the crystal spherulites grow in an amorphous matrix enriched in BaO due to phase separation and having a higher BaO content than glass 29.7 H. Indeed TEM (Fig. 3b) shows that crystal growth proceeds undisturbed through the matrix. At 718° C the phase separation develops slowly (Section 3.3) and longer heat treatments than those used here would probably be required if an increased growth rate were to be detected.

These results are regarded as tentative until further work can be done but are in general agreement with those of other authors [29–31].

3.7. Effects of composition changes on nucleation: further discussion

We have established that changes in the matrix composition as a result of phase separation have a marked effect on the crystal nucleation kinetics in this system. The ways in which such changes in composition may influence nucleation were discussed in Part 1. According to classical theory the rate of homogeneous crystal nucleation, I, at a temperature, T, is given by:

$$I = A \exp\left[-(W^* + \Delta G_D)/kT\right] \quad (8)$$

where A is essentially a constant, W^* and ΔG_D are the thermodynamic and kinetic energy barriers, respectively, and k is Boltzmann's constant. For a spherical nucleus $W^* = 16\pi\sigma^3 V_m^2/3\Delta G^2$ where σ is the crystal–liquid interfacial free energy per unit area, V_m is the molar volume of the crystallizing phase, and ΔG is the Gibbs free energy difference (per mole) between the supercooled liquid and the crystal phase. It is often assumed that ΔG_D can be related to viscosity η, so that I is then given by [1, 9]

$$I = (A'/\eta) \exp(-W^*/kT) \quad (9)$$

where A' is a constant.

In principle, viscosity measurements enable the relative importance of the two quantities ΔG_D and W^* to be assessed. Such an approach has been used successfully to interpret the effects of composition on nucleation rates in other systems [1, 9, 32]. Unfortunately there is unsufficient viscosity data to carry out a detailed analysis in the $BaO–SiO_2$ system (Section 3.5). However, some approximate comparisons can be made. The data in Fig. 16 indicate a fall in viscosity with increase in BaO content. Assuming glasses 27 and 28.3 A had phase separated at 732° C, their matrix compositions would be about 30.8 mol % BaO [17]. Their viscosities were about twice that of the barium disilicate glass. A similar ratio of viscosities would be expected at temperatures other than 732° C. However I in the phase-separated glass 28.3 A (Fig. 5) was $26.5\,mm^{-3}\,sec^{-1}$, about 17 times lower than in the glass 33.3 A at 745° C (see [8]). Thus the difference in nucleation rates cannot be explained solely in terms of a change in viscosity (and hence ΔG_D). A large part of the change in I appears to be caused by an alteration in W^*.

Alternatively, the effect of the kinetic barrier ΔG_D may be determined from crystal growth rate measurements. According to theory [9], at high undercoolings (i.e. for the temperature range used in this work) the growth rate U is controlled predominantly by the kinetic barrier to growth $\Delta G'_D$ and is proportional to $\exp(-\Delta G'_D/kT)$. Making the tentative assumption that $\Delta G_D = \Delta G'_D$, i.e. the atomic transport processes in nucleation and in growth are the same, changes in U with composition at a given temperature may be used to calculate changes in ΔG_D. If we examine the growth rate data in Table III it is evident that the growth rate in glass 33.3 A at 745° C was about three times higher than in the phase-separated glass 28.3 A. Again, this factor is much lower than the ratio of nucleation rates in these two glasses at 745° C, and the change in I cannot be caused simply by a variation in ΔG_D.

We thus conclude that both ΔG_D and W^* play an important role in governing the effect of composition on nucleation rates, although W^* has the larger effect. W^*, in turn, depends on σ and ΔG. In principle, changes in both of these quantities contribute to the variation in W^* with composition. Thus ΔG should increase as the glass approaches the stoichiometric $BaO \cdot 2SiO_2$ composition. Also it is reasonable to assume that σ is lower the closer the compositions of the glass and nucleating phase because the parent glass and crystal phase are then more structurally similar

[5]. As we have seen, these factors and the decrease in viscosity as the barium disilicate composition is approached account for the much higher nucleation rates in the $BaO \cdot 2SiO_2$ glass than in the other compositions (higher in silica) and explain the increase in nucleation rates with time in the glasses undergoing amorphous phase separation.

It is of interest to compare briefly the present results with the recent work of Zanotto and James [27] on the Li_2O-SiO_2 system. They found that for glasses undergoing amorphous phase separation the crystal nucleation rates increased with time of heat treatment because of a shift in matrix composition, in exactly the same manner to the $BaO-SiO_2$ system. However, the $Li_2O \cdot 2SiO_2$ glass, outside the immiscibility region, had a lower crystal nucleation rate than in the fully phase separated glasses, a result in striking contrast to the $BaO-SiO_2$ system where the barium disilicate glass had the highest rates. This behaviour was explained as follows. The crystalline phase precipitated in the phase separated glasses was a solid solution which differed significantly in composition from the stoichiometric lithium disilicate phase precipitated in the $Li_2O \cdot 2SiO_2$ glass. It was therefore likely that the thermodynamic driving force (ΔG) for crystallization was higher for the phase-separated glasses than for the $Li_2O \cdot 2SiO_2$ glass, giving higher nucleation rates for the former glasses. It is easily shown that such an effect on ΔG could occur from consideration of the probable shape of the free energy against composition curve for the solid solution phase. Another possibility is that the interfacial energy σ is lower for the phase-separated glasses, but the effect on ΔG appears the most likely. It would appear that in the $BaO-SiO_2$ system such effects either do not occur or are of minor importance, and that the earlier simpler interpretation applies.

4. Conclusions

$BaO-SiO_2$ glasses containing 27.0, 28.3, 29.7, 29.9 and 33.3 mol % BaO were melted and homogenized in electric furnaces. The major components and levels of minor impurities in the glasses were thoroughly analysed. The results of analysis were close to the nominal compositions. Most of the glasses contained 0.3 wt % SrO as the main impurity, the source being the $BaCO_3$ batch material. The total level of other impurities was about 0.1 wt %. The glasses were highly homogeneous, the homogeneity being carefully checked by measuring the uniformity of crystal nucleation in different samples.

The kinetics of volume nucleation (probably homogeneous) of the barium disilicate crystal phase were determined by quantitative optical microscopy in the glasses. The results were correlated with small-angle X-ray scattering (SAXS) studies of the kinetics of amorphous phase separation in the glasses and with transmission electron microscopy (TEM).

SAXS showed that amorphous phase separation developed rapidly in glasses containing 27.0 and 28.3 mol % BaO after heating at 743° C and 760° C. The average diameters D of the amorphous particles were determined from the slopes of Guinier plots of the SAXS intensities. The plots were linear over a large angular range indicating narrow size distributions. The average diameters, D, increased with time, t, of isothermal treatment according to well established laws for the early and more advanced stages of phase separation (including $D \propto t^{1/3}$, as expected for diffusion-controlled Ostwald ripening in the later stages). The D values were in reasonable agreement with the diameters measured by thin foil TEM. The integrated SAXS intensity, Q, showed that the equilibrium composition of the matrix was attained after 3 to 4 h at 760° C and after about 7 h at 743° C for the glass 28.3. For glass 27.0 it was attained in less than 2.5 h. The number of silica-rich droplets and their specific surface area decreased from the earliest stage of heat treatment, indicating that in these samples most of the nucleation of droplets occurred during cooling from the melt or within a short period of heat treatment. These observations demonstrated that the coarsening stage began well before the attainment of the equilibrium matrix composition, a result of considerable interest.

TEM revealed fine-scale amorphous phase separation in glasses 27.0 and 28.3 after heating at 743° C and above. As-quenched specimens of glass 28.3 showed no detectable phase separation by TEM. No phase separation could be detected by TEM in glasses 29.7 and 29.9 even when they were heated at temperatures (such as 743° C) just within the miscibility gap. This was probably caused by an insufficiently large thermodynamic free energy driving force, ΔG, for nucleation of droplets, as observed in other studies. TEM showed that the crystalline barium disilicate needles grew through the amorphous baria-rich matrix in the phase separated glass 28.3 heated at 743° C apparently leaving the silica-rich droplets undisturbed.

For glasses 27 and 28.3 a striking correlation was found at two temperatures (743 and 760° C) between the times required for the amorphous (baria-rich) matrix to reach the equilibrium composition, revealed by a constant value of the integrated SAXS intensity Q, and the period of increasing crystal nucleation rates in glasses undergoing amorphous phase separation. The crystal nucleation rates in glasses that did not phase separate (such as 29.7 and 29.9) were constant with time at all temperatures studied. In the phase separated glasses no correlation was found between the nucleation rates of crystals and the interfacial area and number of the amorphous droplets determined by SAXS.

The phase-separated glasses with 27.0 and 28.3 mol % BaO showed nearly identical crystal nucleation rates at the same temperatures. Again there was no direct correlation between the volume fraction and specific surface area of the amorphous droplets with the crystal nucleation rates in these glasses. These observations indicate that the crystal nucleation rates depend mainly on the composition of the baria-rich matrix because the baria content in the matrix was the same for glasses 27.0 and 28.3 after phase separation at the same temperature.

The crystal nucleation rates increased with the BaO content for the non-phase separated glasses. In the phase-separated glasses, the crystal nucleation rates increased with the BaO content in the matrix (baria-

rich) phase. The stoichiometric $BaO \cdot 2SiO_2$ glass gave the highest nucleation rates as expected from theoretical considerations [5].

The main conclusions from these nucleation studies are that the enhanced nucleation rates observed for glasses undergoing phase separation are caused predominantly by enrichment in BaO of the matrix phase, and that there is no direct relation between the morphology of phase separation and crystal nucleation in $BaO-SiO_2$ glasses. These conclusions are in excellent agreement with those of Parts 1 and 2.

An additional, less obvious, effect was detected in certain of the N_v against time plots. In some cases an inflexion was observed corresponding to a temporary maximum in the nucleation rate dN_v/dt, the effect disappearing at longer times. These inflexions occurred when the amorphous phase separation was in the early stages (before attainment of the equilibrium composition of the matrix). They may be caused by some preferential nucleation (possibly heterogeneous) within the diffusion zones (silica depleted regions) which exist around the amorphous droplets in the earlier stages of their growth. This is a minor effect because the inflexions are more pronounced at higher temperatures where the homogeneous nucleation rates are lower. They appear to be masked and undetectable at temperatures where the homogeneous rate is high (i.e. in the region of 700° C).

The viscosities of glasses 27.0, 28.3 and 29.9 at a given temperature were equal within experimental error reflecting the similarity of the BaO content in the matrix phases of the phase-separating glasses 27.0 and 28.3 and in the non-separating glass 29.9. The barium disilicate glass had a lower viscosity.

Some measurements of crystal growth rates in phase-separated and non-phase separated glasses indicated that the crystal growth rate was increased by an increase in the BaO content in the matrix resulting from amorphous phase separation, in a similar way to the effects of matrix composition on the crystal nucleation rate.

The viscosity and crystal growth rate measurements in different glasses were used to determine the variation with composition of the term $\exp(-\Delta G_D/kT)$ in the classical equation for nucleation rate (ΔG_D is the kinetic nucleation barrier). Comparisons with the crystal nucleation rates indicated that changes in both ΔG_D and W^*, the thermodynamic barrier, with BaO content have a significant influence on the variation of the nucleation rates. However, changes in W^* have the larger effect.

Finally, while the present study shows that amorphous phase separation has an important role in the formation of glass ceramics, and the conclusions should be valid in principle for all systems, caution should be exercised when generalizing these results to more complex multi-component systems. Thus the observed increase in nucleation rates as a result of phase separation are relatively small (one order of magnitude or less) when compared with the effect of nucleating agents (such as TiO_2, P_2O_5 and ZrO_2) which can increase the nucleation rates by many orders of magnitude in certain systems. The roles of these nucleating agents are frequently complex. They often promote immiscibility as well as high crystal nucleation rates. However, it should not be assumed that amorphous phase separation necessarily plays a major part in their action, as is evident when considering the effect of adding P_2O_5 to Li_2O-SiO_2 glasses [1].

Acknowledgements

Thanks are due to Mr M. Wilson, University of Sheffield, for carrying out the EPMA work, and to Mr A. Bachega, Universidade Federal de São Carlos, for performing some of the gravimetric analyses.

References

1. P. F. JAMES, in "Nucleation and Crystallization in Glasses", Advances in Ceramics, Vol. 4, edited by J. H. Simmons, D. R. Uhlmann and G. H. Beall (The American Ceramic Society, Columbus, Ohio, 1982)pp. 1–48.
2. P. W. McMILLAN, "Glass Ceramics", 2nd Edn (Academic, London, 1979).
3. P. F. JAMES, *J. Mater. Sci.* **10** (1975) 1802.
4. A. F. CRAIEVICH, E. D. ZANOTTO and P. F. JAMES, *Bull. Minéral.* **106** (1983) 169.
5. A. H. RAMSDEN and P. F. JAMES, *J. Mater. Sci.* **19** (1984) 1406.
6. *Idem, ibid.* **19** (1984) 2894.
7. E. D. ZANOTTO, PhD thesis, University of Sheffield, (1982).
8. E. D. ZANOTTO and P. F. JAMES, *J. Non-Crystalline Solids* **74** (1985) 373.
9. C. J. R. GONZALEZ-OLIVER, P. S. JOHNSON and P. F. JAMES, and P. F. JAMES, P. F. JAMES, *J. Mater. Sci.* **14** (1979) 1159.
10. W. LUZATTI, *Acta Crystallogr.* **13** (1960) 939.
11. A. GUINIER and G. FOURNET, "Small Angle Scattering of X-rays" (Wiley, New York, 1955).
12. G. POROD, *Z. Kolloid* **124** (1951) 83.
13. *Idem, ibid.* **125** (1952) 51.
14. *Idem, ibid.* **133** (1953) 16.
15. R. W. DOUGLAS, W. L. ARMSTRONG, J. P. EDWARD and D. HALL, *Glass Tech.* **6** (1965) 52.
16. E. D. ZANOTTO, *Ceramica* **29** (1983) 135.
17. W. HALLER, D. H. BLACKBURN and J. H. SIMMONS, *J. Am. Ceram. Soc.* **57** (1974) 120.
18. D. G. BURNETT and R. W. DOUGLAS, *Phys. Chem. Glasses* **11** (1970) 125.
19. T. P. STEWARD III, D. R. UHLMANN and D. TURNBULL, *J. Amer. Ceram. Soc.* **51** (1968) 278, 634.
20. G. F. NEILSON, *Discuss. Faraday Soc.* **50** (1970) 145.
21. V. GEROLD, "Small Angle X-ray Scattering", edited by H. Brumberger (Gordon and Breach, New York, 1967) p. 277.
22. W. S. ROTHWELL, *J. Appl. Phys.* **39** (1968) 1840.
23. M. TOMOZAWA, *Phys. Chem. Glasses* **13** (1972) 161.
24. E. D. ZANOTTO, A. F. CRAIEVICH and P. F. JAMES, *J. Physique* **43** (1982) C9, 107.
25. D. H. KIRKWOOD, *Acta Metall.* **18** (1970) 563.
26. P. DEBYE, H. R. ANDERSON, H. BRUMBERGER, *J. Appl. Phys.* **28** (1957) 679.
27. E. D. ZANOTTO and P. F. JAMES, Proceedings of the 13th International Glass Congress, Hamburg, 1983 (Glastechnische Berichte, Frankfurt, 1983) p. 794.
28. E. D. ZANOTTO and A. F. CRAIEVICH, *J. Mater. Sci.* **16** (1981) 973.
29. T. OGURA, R. HAYAMI and M. KADOTA, *J. Ceram. Soc. Jpn.* **76** (1968) 277.
30. M. TOMOZAWA, *Phys. Chem. Glasses* **14** (1973) 112.
31. A. H. RAMSDEN, PhD thesis, University of Sheffield, (1977).
32. C. J. R. GONZALEZ-OLIVER, PhD thesis, University of Sheffield (1979).

Received 13 September
and accepted 12 October 1985